The TOR signaling pathway regulates vegetative development, aflatoxin biosynthesis, and pathogenicity in *Aspergillus flavus*

Guoqi Li, Xiaohong Cao, Elisabeth Tumukunde, Qianhua Zeng, Shihua Wang*

Key Laboratory of Pathogenic Fungi and Mycotoxins of Fujian Province, Key Laboratory of Biopesticide and Chemical Biology of Education Ministry, and School of Life Sciences, Fujian Agriculture and Forestry University, Fuzhou, 350002, China.

Corresponding author:
Name: Shihua Wang Professor
School of Life Sciences,
Fujian Agriculture and Forestry University
Fuzhou, Fujian, 350002, China
Phone/Fax: +86-591-83789312
E-mail: wshyyl@sina.com

These authors contributed equally to this work.

Abstract

The target of rapamycin (TOR) signaling pathway is highly conserved and plays a crucial role in diverse biological processes in eukaryotes. However, the underlying mechanism of the TOR pathway in *A. flavus* remains elusive. In this study, we identified and characterized nine genes encoding various components of the TOR pathway in *A. flavus,* and investigated their biological function. The FK506-binding protein Fkbp3 and its lysine succinylation are important for aflatoxin production and rapamycin resistance. The Tor kinase plays a pivotal role in the regulation of growth, spore production, aflatoxin biosynthesis, and osmotic and rapamycin stress. As a significant downstream effector molecule of the Tor kinase, the Sch9 kinase regulates aflatoxin B_1 (AFB_1) synthesis, osmotic and calcium stress response in *A. flavus,* and this regulation is mediated through its S_TKc, S_TK_X domains, and the ATP binding site at K340. We also showed that the Sch9 kinase may have a regulatory impact on the high-osmolarity glycerol (HOG) signaling pathway. TapA and TipA, the other downstream components of the Tor kinase, play significant roles in regulating sclerotia formation and cell wall stress response in *A. flavus*. The members of the TapA-phosphatase complexes, SitA and Ppg1, are crucial for various biological processes in *A. flavus*, including vegetative growth, sclerotia formation, AFB_1 biosynthesis, and pathogenicity. Furthermore, we showed that SitA and Ppg1 are involved in regulating lipid droplets (LDs) biogenesis and cell wall integrity (CWI) signaling pathway. In addition, another phosphatase complex, Nem1/Spo7, plays

critical roles in hyphal development, conidiation, aflatoxin, and lipid droplets biogenesis. This study provides an important insight into the regulatory network of the TOR signaling pathway and the molecular mechanism of aflatoxin biosynthesis in *A. flavus*.

Keywords: *Aspergillus flavus*; the TOR signaling pathway; aflatoxin; vegetative development

Introduction

Aspergillus flavus is one of the most important phytopathogenic fungi that frequently contaminates various plants, causing economic losses in agricultural commodities and posing serious health concerns in developing countries [1]. *A. flavus* is also an opportunistic human pathogenic fungus that can cause aspergillosis in immune-compromised patients [2]. Aflatoxins (AFs), the toxic and carcinogenic secondary metabolites produced by *A. flavus*, are considered the most potent carcinogen present in nature, causing liver cancer in both humans and animals [3]. The aflatoxin biosynthesis is a complex process involving a series of reactions. Although the majority of the enzyme reactions and genes involved in aflatoxin biosynthesis have been elucidated [4], the related signaling pathway network and specific regulatory mechanisms governing aflatoxin biosynthesis remain elusive. Therefore, exploring the regulatory mechanism of the aflatoxin biosynthesis signaling pathway would provide new insights for preventing *A. flavus* and aflatoxins contamination.

In eukaryotes, the target of rapamycin (TOR) signaling pathway is highly

conserved and plays essential roles in various significant biological processes, including ribosome biosynthesis, cell growth, and autophagy [5]. The serine/threonine-protein kinase Tor serves as a crucial protein component in the TOR signaling pathway, which interacts with other proteins to form multi-protein complexes [6]. In *Saccharomyces cerevisiae*, TOR exists in two distinct multiprotein functional complexes, namely TORC1 and TORC2 [7]. TORC1-mediated signaling governs cellular growth by modulating various growth-related mechanisms and exhibits sensitivity to rapamycin. Conversely, TORC2-mediated signaling primarily regulates cytoskeletal remodeling but remains unaffected by rapamycin [7]. In yeast, there are two *tor* genes, *tor1* and *tor2*, whereas in higher eukaryotes such as plants, animals, and filamentous fungi, there is only one *tor* gene [8-10].

In the fungal kingdom, the TOR signaling pathway has been extensively investigated in three prominent species: the budding yeast *S. cerevisiae* [11-12], the fission yeast *Schizosaccharomyces pombe* [13-15], and the human pathogen *Candida albicans* [16-17]. In *S. cerevisiae*, macrolide antibiotic rapamycin interacts with the cytosolic protein Fkbp12 to form a complex, and the Fkbp12-rapamycin complex effectively inhibits the activity of the Tor kinase function by binding to the FRB domain [18]. The Tap42 phosphatase complexs serves as the primary target of the Tor kinase. Additionally, the Tap42 protein interacts with the Tip41 protein to collaboratively regulate phosphatases, including PP2A and Sit4 [19-20]. Phosphatase Sit4 can dephosphorylate the transcription factor Gln3, regulating the nitrogen source metabolism pathway [21]. In addition, another immediate effector of TORC1 is the

89 AGC kinase Sch9, which participates in various cellular functions processes, such as
90 ribosome biosynthesis, translation initiation, and entry into G_0 phase [22]. The TOR
91 signaling pathway has been documented in various filamentous fungi, including
92 *Fusarium graminearum* [23-24], *Magnaporthe oryzae* [25], *Phanerochaete*
93 *chrysosporium* [26], *Podospora anserine* [27], *A. nidulans* [28], *A. fumigatus* [29-30], *F.*
94 *fujikuroi* [31], *Botrytis cinerea* [32], *F. oxysporum* [33], and *Mucor circinelloides* [34].
95 However, the TOR signaling pathway has not yet been reported in *A. flavus*.

96 In eukaryotic cells, the TOR signaling pathway and the Mitogen Activated Protein
97 Kinase (MAPK) signaling pathways play an important role in regulating adaptive
98 responses to extra- and intracellular conditions [35]. Several studies have demonstrated
99 that the TOR signaling pathway interacts with various other signaling pathways, such
100 as MAPK and CWI. These pathways engage in crosstalk, forming a complex
101 metabolic network that regulates cellular processes [36-40]. However, the underlying
102 mechanisms of multiple crosstalks between the TOR and other signaling pathways in
103 *A. flavus* remain unclear. Therefore, we intended to identify the genes associated with
104 the TOR signaling pathway and elucidate their roles and contributions in regulating
105 vegetative development and aflatoxin biosynthesis in *A. flavus*. Our results
106 demonstrated that the TOR signaling pathway is involved in multiple cellular
107 processes in *A. flavus*. Our findings revealed a complex interplay between the TOR
108 pathway and other signaling pathways (such as HOG and CWI) in *A. flavus*, which
109 play a crucial role in regulating cellular growth and survival under environmental
110 stress conditions.

111 # Results

112 **Rapamycin exhibits inhibitory effects on the growth, sporulation, sclerotia**
113 **formation, and aflatoxin production in *A. flavus***

114 Rapamycin, a secondary metabolite synthesized by *Streptomyces hygroscopicus*,
115 exhibits efficacy in suppressing specific filamentous fungi. In *F. graminearum*,
116 rapamycin has a significant inhibitory impact on growth and asexual reproduction [23].
117 To investigate the effects of rapamycin on vegetative development, sclerotia
118 formation, and secondary metabolism in *A. flavus*, we conducted an assay to
119 determine the sensitivity of the wild-type strain to rapamycin. We observed that the
120 wild-type strain exhibited a high sensitivity to rapamycin. We found that 100 ng/mL
121 of rapamycin significantly inhibited mycelial growth and conidia formation (Fig.1A,
122 1D, 1E). More importantly, the wild-type strain exhibited a significant reduction in
123 sclerotia formation and aflatoxin synthesis (Fig.1B, 1C, 1F, 1G). Additionally,
124 rapamycin resulted in a significant decrease in spore germination rate and sparser
125 conidiophores (Fig. S1A, S1B). These results illustrated that the TOR signaling
126 pathway may be involved in regulating the growth, development, and secondary
127 metabolism in *A. flavus.* Calcofluor white is a chemifluorescent blue dye commonly
128 employed for its nonspecific binding affinity to fungal chitin. Fluorescence
129 microscopy analysis revealed a notable reduction in the blue fluorescence on the cell
130 wall following treatment with rapamycin (Fig.S1C). The intracellular lipid droplets
131 within the hyphae were labeled with BODIPY. We observed that the hyphae treated

132 with rapamycin contained more lipid droplets compared to the control group (Fig.
133 S1D). These findings suggest that the TOR pathway may play important roles in
134 maintaining cell wall integrity and facilitating the biogenesis of lipid droplets.

135 To investigate the potential regulatory role of the TOR pathway in modulating
136 the sporulation, sclerotia formation, and aflatoxin biosynthesis in *A. flavus*, we
137 examined the expression levels of conidia-related, sclerotia formation-related, and
138 aflatoxin-related genes after 3, 6, and 9 hours of treatment with rapamycin. To
139 determine the effects of rapamycin on conidiation, qRT-PCR was conducted to assess
140 the transcript levels of two conidia-related genes, *abaA* and *brlA*. We also conducted
141 qRT-PCR to evaluate the expression levels of three regulators (*nsdC*, *nsdD*, and *sclR*)
142 involved in sclerotia development, and genes involved in AFB_1 biosynthesis, such as
143 the regulatory gene *aflS*, as well as several structural genes (*aflC* and *aflQ*). The
144 strains treated with rapamycin exhibited a significant reduction in the expression
145 levels of genes related to sporulation, sclerotia formation, and aflatoxin synthesis (Fig.
146 1H, 1I, 1J). Overall, these results indicated that the TOR pathway plays a crucial role
147 in regulating the growth, sporulation, sclerotia formation, and aflatoxin biosynthesis
148 in *A. flavus* by modulating the expression of these genes.

149 **The impact of Fkbp3 and its lysine succinylation on AFB_1 biosynthesis and**
150 **rapamycin resistance in *A. flavus***

151 FK506-binding proteins (Fkbps) belong to a highly conserved immunophilin
152 family, which are involved in various cellular functions, such as protein folding,
153 immunosuppression, signaling transduction, and transcription [41]. Fkbps function as

154 molecular switches by binding to target proteins and inducing conformational changes
155 [41]. In *S. cerevisiae*, Fkbp12 and rapamycin interact to form a complex that exerts a
156 negative regulatory effect on the activity of the Tor kinase [42]. The *fkbp12* gene
157 homologue *fprA* in *A. nidulans* shares high levels of homology with that from *S.*
158 *cerevisiae* [28]. According to the protein sequence of FprA from *A. nidulans*, four genes
159 encoding putative proteins with FK506 binding domain, named *fkbp1*
160 (AFLA_126880), *fkbp2* (AFLA_087480), *fkbp3* (AFLA_010910), and *fkbp4*
161 (AFLA_128200), have been identified from the *A. flavus* genome. We generated four
162 *fkbp* knockout strains using homologous recombination, and all *fkbp* disruption strains
163 were confirmed by PCR and sequencing analysis (Fig.S2). Phenotypic analyses
164 showed that the mycelial growth and conidia formation of all the *fkbp* mutants were
165 comparable to the wild-type strain on the PDA medium (Fig. 2A), suggesting that
166 Fkbps have minimal influence on the process of vegetative development. We
167 evaluated AFB_1 synthesis utilizing thin layer chromatography (TLC), and the findings
168 demonstrated a noteworthy reduction in AFB_1 synthesis upon deletion of Fkbp3, in
169 comparison to the wild-type strain (Fig.2B, 2D). Additionally, the quantity of sclerotia
170 exhibited a significant decrease in all *fkbp* mutants compared to the wild-type strain
171 (Fig.S3A, S3B). The aforementioned data indicated that Fkbp3 plays a crucial role in
172 sclerotia formation and aflatoxin biosynthesis in *A. flavus*.

173 To determine the specific Fkbp responsible for rapamycin sensitivity, all mutant
174 strains were cultured on PDA solid plates amended with 100 ng/mL rapamycin. The
175 strain with disrupted *fkbp3* showed significant resistance to rapamycin, while the

176 deletion mutants of *fkbp1*, *fkbp2*, and *fkbp4* did not exhibit any alteration in resistance
177 to rapamycin (Fig.2A, 2C). These results demonstrated that Fkbp3 serves as the
178 principal target for rapamycin in *A. flavus*. In the FK506-sensitivity analysis, we
179 observed a significant suppression of mycelial growth and conidia formation in *A.*
180 *flavus* with the addition of 10 ng/mL FK506 to the PDA medium. Additionally, the
181 deletion of *fkbp3* led to the heightened resistance to FK506 compared to the wild-type
182 strain (Fig.2A, 2C). These findings suggested that Fkbp3 is mainly involved in the
183 modulation of FK506 resistance in *A. flavus*.

184 Previous studies have shown that lysine succinylation plays a significant role in
185 aflatoxin production and pathogenicity in *A. flavus* [43]. Based on the analysis of our
186 succinylome data, we have identified six reliable succinylation sites (K5, K19, K40,
187 K42, K55, and K65) on the Fkbp3 protein. To identify the function of Fkbp3
188 succinylation sites, site-directed mutations were constructed according to the
189 homologous recombination strategy. Compared to the wild-type strain, all point
190 mutants exhibited a comparable phenotype in vegetative growth and conidiation.
191 Interestingly, we observed that the K19A mutation resulted in increased resistance to
192 rapamycin (Fig. 2E, 2F). Additionally, the K19A strain exhibited a significant
193 reduction in the production of AFB_1 compared to the wild-type strain (Fig. 2G, 2H).
194 These findings suggested that the succinylation of Fkbp3 at K19 plays a crucial role in
195 rapamycin resistance and aflatoxin biosynthesis. Furthermore, we found that various
196 point mutants, including K40A, K42A, and K55A, exhibited reduced levels of AFB_1
197 production in comparison to the wild-type strain (Fig. 2G, 2H), suggesting that the

198 succinylation of Fkbp3 at other sites also contributes to AFB_1 biosynthesis in *A. flavus*.
199 The above results indicated that the K19 site likely plays a more prominent role in
200 Fkbp3 succinylation compared to other sites.

201 **The Tor kinase** plays a critical role **in *A. flavus***

202 In *S. cerevisiae*, the Tor kinase can interact with a diverse range of proteins,
203 resulting in the formation of complex structures known as TORC1 and TORC2 [44].
204 TORC1 can detect various signals, including nutrients, growth factors, and
205 environmental stress. It plays a crucial role in regulating cellular processes such as
206 gene transcription, protein translation, ribosome synthesis, and autophagy [45]. To
207 identify the ortholog of the Tor protein in *A. flavus*, the *S. cerevisiae* Tor protein was
208 utilized as search queries in the *A. flavus* genome database using the Basic Local
209 Alignment Search Tool (https://blast.ncbi.nlm.nih.gov/Blast.cgi). The genome of *A.*
210 *flavus* contains a solitary ortholog of the *tor* gene (AFLA_044350), which encodes a
211 protein exhibiting 48.91% similarity to *S. cerevisiae* Tor2. We used the absolute
212 quantitative PCR technique to identify the copy number of the *tor* gene at the genome
213 level in *A. flavus* (Table S1). To elucidate the function of the Tor kinase in *A. flavus*,
214 we employed gene deletion techniques to target the *tor* gene. While our attempt to
215 obtain a null mutant was unsuccessful, we constructed a single copy deletion strain,
216 *tor*+/-, through homologous recombination, which contains one copy of the *tor* gene
217 (Table S1). Compared to the wild-type strain, the *tor*+/- strain exhibited a
218 significantly slower growth rate on PDA (Fig. 3C). Additionally, the *tor*+/- strain
219 produced fewer conidia and sclerotia compared to the wild-type strain (Fig. 3B, S4).

220 The results from thin-layer chromatography (TLC) revealed a noteworthy decrease in
221 AFB_1 synthesis in the *tor*+/- strain compared to the wild-type strain (Fig. 3D, 3F).
222 Interestingly, the *tor*+/- mutant exhibited a notable increase in sensitivity to
223 rapamycin and decreased sensitivity to osmotic stress (Fig. 3C, 3E, S5). Furthermore,
224 the qRT-PCR results demonstrated a significant downregulation in the expression
225 levels of the genes associated with sexual sporulation and aflatoxin synthesis in the
226 *tor*+/- mutant compared to the wild-type strain (Fig. S6). The transcriptional level of
227 the *tor* gene in the *tor*+/- mutant was downregulated compared to the level in the
228 wild-type strain (Fig. S6). These findings suggested that the Tor kinase plays a crucial
229 role in various biological processes in *A. flavus*, including vegetative growth, asexual
230 development, sclerotia formation, response to environmental stress, and biosynthesis
231 of aflatoxins.

232 The Tor protein is characterized by the presence of various conserved domains,
233 including the DUF3385, FAT, FKBP12-rapamycin binding (FRB), kinase catalytic,
234 and FATC domains, which are located at the N-terminus (Fig. 3A). To investigate the
235 functional significance of the FRB domain within the Tor kinase, the FRB domain
236 was eliminated using homologous recombination. Compared to the *tor*+/- strain, the
237 $tor^{\Delta FRB}$ mutant displayed comparable deficiencies in vegetative growth, conidiation,
238 sclerotia formation, osmotic stress, and rapamycin sensitivity (Fig. 3B, 3C, S4, S5).
239 Based on these observations, we speculated that the FRB domain plays a pivotal role
240 in the modulation of the Tor kinase activity, thereby influencing fungal development
241 and rapamycin resistance in *A. flavus*.

242 **The Sch9 kinase is involved in aflatoxin biosynthesis and the HOG pathway**

243 Sch9, a Ser/Thr kinase belonging to the AGC family, is directly phosphorylated by
244 TORC1. The phosphorylation of Sch9 is inhibited by rapamycin, as well as by carbon
245 or nitrogen starvation [22]. The putative *sch9* gene (AFLA_127440) in *A. flavus*
246 encodes a protein consisting of 706 amino acids, exhibiting 80.31% identity to the
247 Sch9 protein in *A. nidulans*. To investigate the role of Sch9 in *A. flavus*, we attempted
248 to create a *sch9* deletion mutant using a homologous recombination strategy. The
249 Δ*sch9* strain exhibited typical vegetative growth and conidiation similar to the
250 wild-type strain (Fig. 4B). TLC assay and quantitative analysis showed a significantly
251 decreased aflatoxin production in the Δ*sch9* strain compared to the wild-type strain
252 (Fig. 4C, 4G). These results indicated that Sch9 regulates aflatoxin biosynthesis in *A.*
253 *flavus*.

254 In yeast, Sch9 plays an important role in the transcriptional activation of
255 osmostress inducible genes [46]. To characterize the roles of Sch9 in stress response,
256 we examined the sensitivity of the *sch9* deletion strain to various stresses including
257 osmotic stress and calcium stress. Compared with the wild-type strain, the Δ*sch9*
258 mutant significantly increased sensitivity to calcium stress (Fig. S7), and decreased
259 sensitivity to osmotic stress induced by NaCl and KCl (Fig.4D, 4H). In *A. flavus*, the
260 Sch9 kinase consists of several domains, including the protein kinase C conserved
261 region 2 (C2), protein kinase (S_TKc), AGC-kinase C-terminal (S_TK_X) domain,
262 and an ATP binding site (Fig. 4A). To explore the role of these domains and the ATP
263 binding site in Sch9 kinase, we constructed deletion strains for both domains and a

264 *sch9*^{K340A} mutant. The results revealed that the *sch9*$^{\Delta S_TKc}$ strain, *sch9*$^{\Delta S_TK_X}$ strain, and
265 *sch9*^{K340A} mutant exhibited similar phenotypes in osmotic stress and AFB_1 production
266 as the Δ*sch9* mutant (Fig.4B, 4C, 4D). Therefore, we speculate that the protein kinase
267 domain, kinase C-terminal domain, and the ATP binding site at K340 play a crucial
268 role in modulating the impact of Sch9 on aflatoxin biosynthesis and stress response in
269 *A. flavus*.

270 To investigate the potential function of Sch9 in the HOG and TOR pathways in *A.*
271 *flavus*, we conducted a sensitivity analysis of the Δ*sch9* strain to rapamycin.
272 Compared to the wild-type strain, the *sch9* deletion strain exhibited a slightly higher
273 sensitivity to rapamycin (Fig. 4B, 4F). The MAKP Hog1 is an element of the high
274 osmolarity glycerol (HOG) pathway. To verify the connection between Sch9 and the
275 HOG-MAPK pathway, the phosphorylation levels of Hog1 kinase were measured
276 under osmotic stress (1M NaCl). Western blot analysis showed that the
277 phosphorylation level of Hog1 increased significantly in the Δ*sch9* strain (Fig. 4E).
278 This finding suggested that Sch9 plays a pivotal role in modulating the response of
279 Hog1 to osmotic stress. Taken together, these results reflected that Sch9 regulates
280 osmotic stress response via the HOG pathway in *A. flavus*.

281 **TapA and TipA participate in regulation of sclerotia development and cell wall**
282 **stress response**

283 Tap42, a protein that associates with phosphatase 2A, serves as the direct target of
284 the Tor kinase in yeast. Tap42 plays a crucial role in various Tor functions,
285 particularly in the regulation of transcriptional processes [47]. The genome of *A. flavus*

286 contains a homolog of *tap42* named *tapA* (AFLA_092770), which is predicted to
287 encode a 355 amino-acid protein (sharing 31.9% identity with *S. cerevisiae* Tap42).
288 To further determine the function of the TapA regulator in the TOR signaling pathway
289 of *A. flavus*, we conducted targeted gene deletion experiments on *tapA*. We failed to
290 obtain a null mutant, therefore we generated the *tapA+/-* strain, which contains one
291 copy of the *tapA* gene (Table S2). Compared to the wild-type strain, the *tapA*+/- strain
292 exhibited diminished hyphal growth and conidiation (Fig. 5A, 5C), indicating that
293 TapA is important for vegetative growth and conidiation. The results of the rapamycin
294 sensitivity test indicated that the *tapA+/-* strain displayed reduced sensitivity to
295 rapamycin (Fig.5A, 5E). In addition, the *TapA*+/- strain was unable to generate any
296 sclerotia (Fig. 5B, 5F), and almost lost its capability in AFB_1 production compared to
297 the wild-type strain (Fig. 5D, 5G), these findings indicated that TapA is essential for
298 sclerotia formation and biosynthesis of AFB_1. The *tapA*+/- mutant was more
299 insensitive to cell wall stress, including CFW and CR (Fig. S8). Furthermore, the
300 levels of *nsdC*, *nsdD*, and *sclR* expression were significantly decreased in *tapA*+/-
301 strain compared to those in the wild-type strain (Fig. S9). The transcriptional level of
302 the *tapA* gene in the *tapA*+/- strain was drastically downregulated compared to the
303 wild-type strain (Fig. S9). These findings have demonstrated the significantly positive
304 impact of TapA on the growth, sporulation, sclerotia formation, cell wall stress, and
305 AF biosynthesis in *A. flavus*.

306 In *S. cerevisiae*, Tip41 was identified as a Tap42-interacting protein and has been
307 measured to function as a negative regulator of Tap42, which downregulates TORC1

308 signaling via activation of PP2A phosphatase [48]. The putative orthologue of *tip41* in
309 *A. flavus* named *tipA* (AFLA_047310). The amino acid sequence of TipA exhibits a
310 similarity of 40.49% to Tap41 in *S. cerevisiae*. To elucidate the function of the TOR
311 signaling pathway protein TipA in *A. flavus*, we generated the *tipA* deletion mutants.
312 The Δ*tipA* strain exhibited a slightly reduced number of conidia produced on PDA
313 compared to the wild-type strain (Fig. 5A). Meanwhile, the Δ*tipA* strain exhibited
314 decreased sensitivity to rapamycin (Fig. 5A). The Δ*tipA* strain was unable to produce
315 any sclerotia (Fig. 5B). In addition, the Δ*tipA* strain was more sensitive to cell wall
316 and cell membrane stress, including CR and SDS (Fig. S8). Additionally, the
317 expression levels of *nsdC* and *nsdD* exhibited a decrease in Δ*tipA* strain compared to
318 the wild-type strain (Fig. S9). These results indicated that TipA is crucial for the
319 sclerotial formation and cell wall stress in *A. flavus*.

320 **Phosphatase SitA and Ppg1 are involved in growth, conidiation, and sclerotial**
321 **formation**

322 In *S. cerevisiae*, Tap42 has been identified to interact with the catalytic subunit of
323 type 2A protein phosphatases, including Pph3, Pph21, and Pph22, as well as the type
324 2A-like phosphatases Sit4 and Ppg1[19]. Phosphatase *sitA* (AFLA_108450) and *ppg1*
325 (AFLA_132610) were identified in *A. flavu*s, encoding putative orthologs of *sit4* and
326 *ppg1* in *S. cerevisiae.* To determine the biological functions of phosphatase SitA and
327 Ppg1 in *A. flavu*s, we disrupted the *sitA* and *ppg1* by homologous recombination
328 strategy. To further investigate the relationship between phosphatase SitA and Ppg1,
329 we additionally generated complemented and double deletion mutants. The vegetative

330 development phenotype analysis showed that the Δ*sitA*, Δ*ppg1*, and Δ*sitA*/Δ*ppg1*
331 strains grew significantly more slowly than the wild-type strain on PDA (Fig. 6A, 6D).
332 Additionally, the Δ*sitA*, Δ*ppg1*, and Δ*sitA*/Δ*ppg1* strains were more sensitive to
333 rapamycin (Fig. 6A, 6E). In addition, the Δ*sitA*, Δ*ppg1*, and Δ*sitA*/Δ*ppg1* strains
334 formed lower number of conidiophores (Fig. 6A). To gain further insight into the role
335 of SitA and Ppg1 in the process of conidiation, qRT-PCR was employed to determine
336 the transcript levels of conidial synthesis-related genes (*abaA* and *brlA*). The
337 expression levels of the *abaA and brlA* genes were significantly downregulated in the
338 Δ*sitA*, Δ*ppg1*, and Δ*sitA*/Δ*ppg1* mutants when compared to the wild-type and
339 complemented strains (Fig. 6G). The analysis of sclerotial formation revealed that the
340 Δ*sitA*, Δ*ppg1*, and Δ*sitA*/Δ*ppg1* mutants exhibited a complete inability to produce any
341 sclerotia (Fig. 6B). To further prove these findings, we conducted qRT-PCR to
342 determine the expression levels of three regulators (*nsdC*, *nsdD*, and *nclR*) of sclerotia
343 development. Our findings indicated that the expression levels of *nsdC*, *nsdD*, and
344 *sclR* were all significantly reduced in the Δ*sitA*, Δ*ppg1*, and Δ*sitA*/Δ*ppg1* mutants (Fig.
345 6H), which is consistent with the observed decrease in sclerotia production in the
346 Δ*sitA*, Δ*ppg1*, and Δ*sitA*/Δ*ppg1* mutants. These results showed that SitA and Ppg1 are
347 crucial for hyphal development, conidiation, and sclerotia formation in *A. flavus*.

348 **SitA and Ppg1 play crucial roles in aflatoxin biosynthesis and pathogenicity**

349 We assayed AFB_1 biosynthesis in the Δ*sitA*, Δ*ppg1*, and Δ*sitA*/Δ*ppg1* mutants.
350 TLC analyses revealed that the Δ*sitA* and Δ*sitA*/Δ*ppg1* strains exhibited a decrease in
351 AFB_1 production, whereas the Δ*ppg1* strain showed a significant increase in AFB_1

352 production compared to the wild-type and complemented strains (Fig. 6C, 6F). The
353 expression levels of genes related to aflatoxin synthesis, including structural genes
354 (*aflO* and *aflP*) and regulatory genes (*aflR* and *aflS*), were determined by qRT-PCR in
355 the Δ*sitA*, Δ*ppg1*, and Δ*sitA*/Δ*ppg1* mutants. The results revealed a significant
356 downregulation of these genes in the Δ*sitA* and Δ*sitA*/Δ*ppg1* mutants, while
357 upregulated in the Δ*ppg1* mutants, compared to the wild-type and complemented
358 strains (Fig. 6I). These results indicated that SitA and Ppg1 play different roles in
359 regulating aflatoxin biosynthesis in *A. flavus*.

360 We conducted pathogenicity tests on peanuts and maize to examine the
361 pathogenicity of the phosphatases SitA and Ppg1 on crops. The results showed that
362 the wild-type and complemented strains demonstrated complete virulence on all
363 peanut and maize seeds. In contrast, the Δ*sitA*, Δ*ppg1*, and Δ*sitA*/Δ*ppg1* mutants
364 displayed compromised colonization on peanut and maize seeds (Fig. 7A). In addition,
365 the number of conidial productions in these mutants on the infected peanut seeds also
366 dramatically decreased compared to those of the wild-type and complemented strains
367 (Fig. 7C). The thin-layer chromatography analyses revealed that the Δ*ppg1* mutant
368 exhibited increased production of AFB_1 in peanuts and maize. Conversely, the levels
369 of aflatoxin produced by the Δ*sitA* and Δ*sitA*/Δ*ppg1* mutants on peanut and maize
370 were significantly reduced compared to the the wild-type and complemented strains
371 (Fig. 7B, 7D). This observation aligns with the above results of aflatoxin biosynthesis
372 from all mutant strains in the YES medium. All these data showed that SitA and Ppg1
373 are crucial for crop seeds' pathogenicity.

374 **SitA and Ppg1 are involved in regulating cell wall integrity**

375 To explore the role of phosphatases SitA and Ppg1 in response to cell wall stress,
376 all strains were cultivated on PDA amended with CFW, CR, and SDS. We found that
377 the relative growth inhibition of Δ*sitA*, Δ*ppg1* and Δ*sitA*/Δ*ppg1* mutants induced by
378 cell wall stress were significantly increased compared to the wild-type and
379 complemented strains (Fig. 8A, 8B). Further investigations using qRT-PCR revealed a
380 notable reduction in the expression levels of genes related to the synthesis of cell
381 walls, specifically chitin synthase genes *chsA*, *chsD*, *chsE*, and *β-1,6*, in the Δ*sitA*,
382 Δ*ppg1*, and Δ*sitA*/Δ*ppg1* strains (Fig. 8C). Western blot analysis also revealed that the
383 phosphorylation level of Slt2 was significantly elevated in the Δ*sitA*, Δ*ppg1*, and
384 Δ*sitA*/Δ*ppg1* strains under cell wall stress (200 μg/ml CFW) (Fig. 8D). In conclusion,
385 the phosphatases SitA and Ppg1 play a crucial role in regulating cell wall integrity.

386 **The phosphatase complex Nem1/Spo7 are important for growth, aflatoxin**
387 **biosynthesis, and LD biogenesis**

388 Lipid droplets (LDs) are highly dynamic spherical organelles, which appear in
389 the cytosol of most eukaryotic cell types[49]. Rapamycin treatment led to the
390 accumulation of lipid droplets in various filamentous fungi [24]. The FgTOR pathway
391 regulates the phosphorylation status of FgNem1 mainly via the
392 FgPpg1/Sit4-FgCak1/other kinase cascade in *F. graminearum* [24]. In this study, we
393 observed that the treatment of hyphae with rapamycin resulted in the accumulation of
394 LD biogenesis (Fig. 9A). This finding suggested that the TOR pathway may regulate
395 the LD biogenesis. However, the underlying regulatory mechanism of LD

396 biosynthesis remain largely unknown in *A. flavus*. To investigate the regulatory
397 mechanism of the TOR pathway in *A. flavus* that controls LD biogenesis, we
398 examined LD accumulation in Δ*sch9*, Δ*sitA*, and Δ*ppg1* mutants. BODIPY staining
399 assays revealed that LD biogenesis was not observed in the Δ*sitA* and Δ*ppg1* strains
400 upon treatment with rapamycin, in contrast to the wild-type and Δ*sch9* strains (Fig.
401 9A, 9B, 9C, 9D). These results indicated that LD biogenesis induced by rapamycin is
402 predominantly reliant on the phosphatases SitA and Ppg1 in *A. flavus*. In *F.*
403 *graminearum*, the phosphatase FgNem1/FgSpo7 complex was involved in the
404 induction of LD biogenesis by rapamycin. Phosphatase *nem1* (AFLA_002649) and
405 *spo7* (AFLA_028590) were identified in *A. flavus*, which encode putative orthologs of
406 *nem1* and *spo7* in *F. graminearum.* To examine the role of the *nem1* and *spo7* genes in
407 *A. flavus*, we generated Δ*nem1* and Δ*spo7* mutants using homologous recombination.
408 The Δ*nem1* and Δ*spo7* mutants displayed a notable reduction in both vegetative
409 growth and conidiation compared to the wild-type strain (Fig. 10A, 10C, 10D). TLC
410 assay revealed a significantly decreased aflatoxin production in the Δ*nem1* and Δ*spo7*
411 compared to the wild-type strain (Fig. 10B). In addition, BODIPY staining showed no
412 visible lipid droplets in the hyphae of Δ*nem1* and Δ*spo7* after rapamycin treatment
413 (Fig. 10E). Taken together, these results indicated that Nem1/Spo7 are involved in
414 vegetative growth, conidiation, aflatoxin production, and LD biogenesis.

415 **Discussion**

416 Aflatoxins (AFs) are a class of toxic secondary metabolites synthesized by *A.*

417 *flavus*, including aflatoxin B_1, B_2, G_1, and G_2, among which AFB_1 has been regarded
418 as the most pathogenic and toxic aflatoxin[50]. Therefore, understanding the regulatory
419 mechanisms involved in fungal secondary metabolites biosynthesis would be
420 instrumental for effectively addressing aflatoxin control in *A. flavus*. In this study, we
421 demonstrated that the target of rapamycin (TOR) signaling pathway plays a pivotal
422 role in regulating growth, sporulation, sclerotia formation, aflatoxin production, and
423 various stress response in *A. flavus*. Through conducting functional studies on genes
424 within the TOR signaling pathway, we explored the conservation and complexity
425 exhibited by the TOR signaling pathway in *A. flavu*s. In addition, we constructed a
426 crosstalk network between the TOR and other signaling pathways (HOG, CWI) and
427 analyzed the specific regulatory process. We proposed that the TOR signaling
428 pathway interacts with multiple signaling pathways, including HOG and CWI
429 pathway, to modulate the cellular responses to diverse environmental stresses (Fig.
430 11).

431 We have observed that rapamycin has a significant impact on the growth and
432 sporulation of *A. flavus* (Fig. 1A). Additionally, it exhibits a strong inhibitory effect on
433 sclerotia production and aflatoxin biosynthesis (Fig. 1B, 1C). The inhibitory effect has
434 been documented in various fungal species, including *Candida albicans* [51],
435 *Cryptococcus neoformans* [51], *Podospora anserine* [27], *A. nidulans* [28], *Magnaporthe*
436 *oryzae* [39], and *F. graminearum* [23]. This suggested that the TOR signaling pathway
437 may have a conserved function in filamentous fungi. The number of FK506-binding
438 proteins varies among different species: there are four Fkbps protein in *S. cerevisiae*

439 and three Fkbps protein in *S. pombe* [52]. In *S. cerevisiae*, rapamycin can bind to Fkbp
440 protein, resulting in the irreversible inhibition of the G_1 phase of the cell cycle and the
441 regulation of cell growth [53]. In *A. nidulans,* the *fkbp12* gene homologue *fprA* displays
442 considerable sequence similarity with homologues identified in the *S. cerevisiae* [28].
443 In this study, based on the homologous alignment of the protein sequence of FprA, it
444 was observed that four *fkbp* genes present in *A. flavus*. Among these, deletion of *fkbp3*
445 exhibited enhanced tolerance to rapamycin (Fig. 2A). So we speculated that
446 rapamycin forms a complex with Fkbp3 in *A. flavus*, subsequently targeting
447 downstream target genes in order to exert its biological function. We found that Fkbp3
448 is involved in sclerotia and aflatoxin biosynthesis in *A. flavus* (Fig. 2A, S3), and
449 subsequent analysis revealed that the underlying mechanism may be associated with
450 succinylation modification. The succinylation sites of Fkbp3 were identified through
451 the utilization of succinylation proteomics data. By constructing point mutant strains
452 and conducting phenotype experiments, we found that the succinylation of Fkbp3 at
453 residue K19 is involved in rapamycin resistance and aflatoxin biosynthesis (Fig. 2E,
454 2G). Previous studies have demonstrated that Fkbp12 has been identified as the
455 receptor for FK506 and rapamycin, which inhibits calcineurin and target of rapamycin
456 complex 1 (TORC1), respectively [53]. The deletion of Fkbp12 confers the resistance
457 to rapamycin in *C. albicans* [51] and *C. neoformans* [51]. The entomopathogenic fungus
458 *Beauveria bassiana* contains three putative *fkbp* genes, and disruption of *Bbfkbp12*
459 significantly increases the resistance to rapamycin and FK506 [54]. The plant
460 pathogenic fungus *F. graminearum* harbors three Fkbps proteins, among which

461 deletion of *Fgfkbp12* leads to resistance to rapamycin [23]. Thus, we propose that these
462 Fkbps may exhibit analogous functionalities in conferring resistance to rapamycin. In
463 *Botrytis cinerea*, deletion of *Bcfkbp12* cause a reduction of the virulence of strain T4,
464 while knockout of the *fkbp12* gene did not affect the pathogenic development of the
465 strain B05.10 [32]. These findings demonstrated that the *fkbp12* homologous genes
466 exhibited conservation in terms of rapamycin resistance. However, there is significant
467 variation in other biological functions among fungal species, which may be attributed
468 to species or strain evolutionary divergence.

469 The Tor kinase functions as a fundamental component of the TOR signaling
470 pathway, which exhibits evolutionary conservation across fungi, plants, and mammals
471 [55]. TOR assembles into two distinct multi-protein complexes known as TORC1 and
472 TORC2. A characteristic that distinguishes TORC1 is its interaction with KOG1
473 (Raptor in mammals) and its sensitivity to the rapamycin-FKBP12 complex [56].
474 Almost all other eukaryotes, including plants, worms, flies, and mammals, have a
475 single *tor* gene, whereas *S. cerevisiae* has two *tor* genes [45]. The Tor kinase is widely
476 conserved both in terms of its structural characteristics and its role as the target of
477 Fkbp-rapamycin. Typically, the Tor kinase exhibits comparable structural
478 characteristics, including the HEAT-like, FAT, FRB, kinase, and FATC domains. The
479 FRB domain is the binding region of the Fkbp-rapamycin complex, and rapamycin
480 resistance is usually caused by the disruption of the FRB domain [45]. The comparison
481 of homology and the analysis of phylogenetics revealed that there is only one
482 predicted *tor* gene in *A. flavus*. To ascertain its functionality, we generated the *tor*

483 single-copy deletion mutant by homologous recombination. We discovered that the
484 Tor kinase is involved in the vegetative growth and asexual development of *A. flavus*
485 (Fig. 3B, 3C). In addition, the *tor*+/- mutant shows a high sensitivity to rapamycin
486 (Fig. 3C). Our findings have demonstrated the significant involvement of Tor kinase
487 and its FRB domain in the processes of morphogenesis, aflatoxin biosynthesis, and
488 multiple stress responses in *A. flavus*. We speculate the common expectation that the
489 deletion of the *tor* and FRB domain should result in insensitivity and resistance to
490 rapamycin，as it disrupts the binding site for Fkbp-rapamycin. However, we observed
491 that the *tor*+/- and FRB domain-deleted mutant were more sensitive to rapamycin.
492 This intriguing result suggests that there are additional factors or complexities
493 involved in TOR signaling pathway regulation in *A. flavus*. We hypothesize that this
494 result is related to the double copy of the *tor* gene. Previous findings demonstrated
495 that the Tor kinase could function as a molecular switch connecting an iron cue to
496 defend against pathogen infection in *C. elegans* [57]. In *A. fumigatus*, the Tor kinase
497 represents a central regulatory node controlling genes and proteins involved in
498 nutrient sensing, stress response, cell cycle progression, protein biosynthesis, and
499 degradation, as well as adaptation to low iron conditions[58]. In summary, the Tor
500 kinase acts as a central regulator in the TOR signaling pathway, playing a crucial role
501 in the regulation of the cell cycle, protein synthesis, and cellular energy metabolism.
502 In *S. cerevisiae*, the protein kinase Sch9 is a major downstream effector of
503 TORC1, and this kinase is known to have crucial functions in stress resistance,
504 longevity, and nutrient sensing [46]. In addition, the TORC1-Sch9 pathway acts as a

505 crucial mediator of chronological lifespan [59]. In filamentous fungi, an intricate
506 network of interactions exists between the TOR and HOG pathways. In *F.*
507 *graminearum* [38], FgSch9 and FgHog1 mutants displayed heightened susceptibility to
508 osmotic and oxidative stresses. The phosphorylation level of FgHog1 increased
509 significantly in FgSch9 mutant. Additionally, the affinity capture-MS assay showed
510 that the Tor kinase was among the proteins co-purifying with FgSch9. These results
511 suggest that FgSch9 serves as an intermediary for the TOR and HOG signaling
512 pathways [38]. Furthermore, FgSch9 plays a crucial role in the regulation of various
513 biological processes such as hyphal differentiation, asexual development, virulence,
514 and DON biosynthesis[38]. In *A. fumigatus*, the SchA mutant was sensitive to
515 rapamycin, high concentrations of calcium and hyperosmotic stress, and SchA was
516 involved in iron metabolism. The SchA mutant exhibited enhanced phosphorylation
517 of SakA in response to osmotic stress [51]. In this study, we discovered that Sch9 is
518 involved in regulating aflatoxin biosynthesis (Fig.4C), and responses to osmotic stress
519 and rapamycin stress (Fig.4B, 4D). The S_TKc domain deletion strain ($sch9^{\Delta S_TKc}$),
520 S_TK_X domain deletion strain ($sch9^{\Delta S_TK_X}$), and $sch9^{K340A}$ mutant displayed a
521 similar phenotype to the Δ*sch9* strain (Fig. 4B, 4C, 4D). These findings revealed that
522 Sch9 plays a significant role in the biological synthesis of aflatoxin and in responding
523 to various stresses. This role is primarily mediated through its kinase domain,
524 kinase-C domain, and ATP binding site k340. We also found that the phosphorylation
525 level of Hog1 increased significantly in the Δ*sch9* strain under osmotic stress (Fig.
526 4E). Based on the above results, we hypothesized that Sch9 was involved in the

527 osmotic stress response by modulating the HOG pathway.

528 In *S. pombe*, the protein Tip41, which interacts with Tap42, plays a significant
529 role in the cellular responses to nitrogen sources by regulating type 2A phosphatases
530 [60]. In *S. cerevisiae*, Tap42-phosphatase complexes associate with TORC1, whereas
531 Tip41 functions to attenuate TORC1 signaling by stimulating the PP2A phosphatase
532 [48]. Unlike its yeast counterpart Tip41, TIPRL, a mammalian Tip41-like protein,
533 exerts a positive influence on mTORC1 signaling by interacting with PP2Ac [61].
534 While the interaction between Tip41 and Tap42 was not observed in the filamentous
535 fungi. The yeast two-hybrid (Y2H) assay showed that FgTip41 interacts with the
536 phosphatase FgPpg1 rather than FgTap42, while the FgTap42 bind with phosphatases
537 FgPp2A, implying that FgTap42, FgPpg1, and FgTip41 form a heterotrimer in *F.*
538 *graminearum* [23]. In the rice blast fungus *M. oryzae*, MoTip41 does not interact with
539 the MoTap42. However, MoTip41 has the ability to bind with the phosphatase
540 MoPpe1, thereby facilitating crosstalk between the TOR pathway and the cell wall
541 integrity pathway [40]. In this study, we found that the TapA and TipA played a crucial
542 role in sclerotia production and cell wall stress in *A. flavus* (Fig. 5B, S8). The *tapA*
543 single-copy deletion mutant and the *tipA* deletion mutant exhibited decreased
544 sensitivity to rapamycin (Fig. 5A). However, the interaction between TapA and TipA
545 is not yet clear in *A. flavus*. We speculated that the interrelations and functions of
546 TapA and TipA in *A. flavus* are comparable to their ortholog in other filamentous
547 fungi.

548 In *S. cerevisiae*, Tap42 can bind and regulate various PP2A phosphatases,

549 including Pph3, Pph21, Pph22, Sit4, and Ppg1. This interaction plays a crucial role in
550 the TOR signaling pathway, particularly in response to rapamycin treatment or
551 nutrient deprivation [48]. The phosphatase Sit4 plays a crucial role in regulating cell
552 growth, morphogenesis, and virulence in *C. albicans* [62]. FgSit4 and FgPpg1 are
553 associated with various cellular processes, including mycelial growth, conidiation,
554 DON biosynthesis, and virulence in *F. graminearum* [23]. In addition, FgSit4 and
555 FgPpg1 are involved in the regulation of various signaling pathways, such as the CWI
556 pathway and lipid droplets biogenesis regulation pathway [23]. In this study, we found
557 that the phosphatase SitA and Ppg1 play critical role in vegetative growth, conidiation,
558 sclerotia formation, and aflatoxin biosynthesis in *A. flavus* (Fig.6A, 6B, 6C).
559 Additionally, the phosphatase SitA and Ppg1 also affect pathogenicity and LD
560 biogenesis (Fig. 7A, 9C, 9D). In addition, TapA/TipA and SitA/Ppg1 exhibits similar
561 functions in sclerotia production and cell wall stress response. Based on these
562 observations, we hypothesized that TapA-phosphatase complexes play a collaborative
563 role in the regulation of the sclerotia formation and cell wall stress response in *A.*
564 *flavus.*

565 After the deletion of the *sitA* and *ppg1* genes, the expression level of genes
566 related to cell wall synthesis has decreased significantly, resulting in damage to the
567 cell wall and showing a higher sensitivity to cell wall integrity stress (Fig. 8C).
568 Western blotting results showed that the phosphorylation level of MAPK kinase Slt2
569 has increased significantly in the Δ*sitA* and Δ*ppg1* strains under cell wall stress,
570 indicating that SitA and Ppg1 exert a negative regulatory effect on the CWI pathway

571 (Fig. 8D). In *M. oryzae*, MoPpe1 and MoSap1 serve as an adaptor complex that
572 connects the CWI and TOR signaling pathways. Activation of the TOR pathway
573 results in the inhibition of the CWI pathway [39]. In addition, the phosphatase MoPpe1
574 interacts with the phosphatase-associated protein MoTip41, facilitating the exchange
575 of information between the TOR and CWI signaling pathways [39]. These results
576 suggest that the phosphatase Ppe1 engages in interactions with various proteins to
577 effectively coordinate the TOR and CWI signaling pathways, thereby regulating the
578 growth and pathogenicity of the rice blast fungus *M. oryzae* [39]. Taken together, we
579 speculated that the phosphatase SitA and Ppg1 might exhibit differential regulation in
580 the CWI and TOR pathways across species in order to fulfill their respective
581 functions.

582 In *F. graminearum,* the phosphatase complex FgNem1/Spo7-FgPah1 cascade
583 plays significant roles in fungal development, DON production, and lipid droplet (LD)
584 biogenesis [24]. In this study, our results indicated that Nem1 and Spo7 are important
585 for vegetative growth and secondary metabolism of *A. flavus* (Fig. 10A, 10B). We
586 have also discovered that LD biogenesis is facilitated by the Nem1/Spo7 and
587 SitA/Ppg1 pathways (Fig. 9C, 9D, 10E). These observations suggest that the PP2A
588 phosphatases play a central role as core phosphatases in the LD biogenesis signaling
589 network. However, it is likely that there are other kinases involved in the regulation of
590 LD biogenesis. To gain a comprehensive understanding of the precise molecular
591 mechanism, further research should focus on investigating the interplay between
592 phosphatases and other kinases.

593 In conclusion, we identified the complex regulatory network that provides insight
594 into the interplay between the TOR, HOG, and CWI signaling pathways, and how
595 they collectively regulate the development, aflatoxin biosynthesis, and pathogenicity
596 of *A. flavus*. By elucidating the functions of genes associated with the TOR signaling
597 pathway, our research could establish a solid foundation for comprehending the
598 molecular mechanism underlying the aflatoxin biosynthesis of *A. flavus*. This, in turn,
599 can provide novel insights into the management of aflatoxin contamination and the
600 mitigation of *A. flavus* infection.

601 # Materials and methods

602 **Strains and cultural conditions**

603 The *A. flavus* strains in this study were shown in Table S3. All strains were
604 cultivated on three different types of agar media: potato dextrose agar (PDA), yeast
605 extract-sucrose agar (YES), and yeast extract-glucose agar (YGT). The growth and
606 conidiation assays were conducted at 37°C. Additionally, aflatoxin production was
607 assessed using YES liquid medium at 29°C.

608 **Constructions of gene deletion and complemented mutants**

609 The construction of gene deletion and complemented strains was carried out
610 using the SOE-PCR strategy, following previously established protocols [63]. The
611 primers utilized for the amplification of the flanking sequences of each gene can be
612 found in Table S3. The putative gene deletion mutants were validated through PCR

613 assays using the appropriate primers (Fig. S2), and their confirmation was
614 subsequently obtained through sequencing analysis.

615 **Detection of *tor* and *tapA* genes copy number in strains**

616 Absolute quantification PCR has been used as a common method for molecular
617 detection of gene copy numbers. According to previous reports, the *sumo* gene is a
618 single-copy gene in *A. flavus*[64]. Following previously established protocols[65], the
619 primers were used to design the amplification of the *sumo* reference gene and *tor* and
620 *tapA* gene. Using *sumo* gene as reference, the *tor* and *tapA* gene copy number was
621 calculated by standard curve.

622 **Growth, conidiation, and sclerotia analysis**

623 To evaluate mycelial growth and conidia formation, 1 μL of 10^6 spores/mL conidia
624 of all strains was point inoculated onto the center of PDA medium, and then cultured
625 at 37°C for 5 days in the dark. The conidia were washed by 0.07% Tween-20 and
626 counted using a hemocytometer and microscope [43]. For sclerotia formation analysis,
627 each strain was inoculated and cultivated on CM agar medium at 37°C in the dark for
628 7 days, and then 75% ethanol was used to wash away mycelia and conidia on the
629 surface of the medium [64]. These assays were repeated at least three times.

630 **Extraction and quantitative analysis of aflatoxin**

631 To extract and quantify aflatoxins (AFs) production, 1 μL of 10^6 spores/mL
632 conidia of all strains was point inoculated onto liquid YES medium and cultures were
633 then incubated at 29°C in the dark for 6 days. AFs were extracted from the media and
634 detected using thin layer chromatography (TLC) [65]. In addition, the standard AFB_1

635 was employed for visual comparison, and AFs were quantitatively analyzed using the
636 Image J tool. The assays were repeated at least three times.

637 **Stress assay**

638 To determine the roles of the gene in *A. flavus* responsing to various
639 environmental stresses, 1 μL of 10^6 spores/mL conidia of all strains were point
640 inoculated onto these PDA solid plates supplemented with various agents. These
641 agents included 1M NaCl, 1M KCl, and 1M $CaCl_2$ for inducing osmotic stress, as
642 well as 100 μg/mL SDS, 200 μg/mL Calcofluor white (CFW), and 200 μg/mL Congo
643 red (CR) for inducing cell wall stress. After 5 days of incubation at 37°C in the dark,
644 the relative rates of inhibition were determined [43]. The assays were repeated at least
645 three times.

646 **Seeds infection assays**

647 To measure the pathogenicity of *A. flavus*, all peanut and maize seeds were
648 washed in 0.05% sodium hypochlorite, 75% ethanol, and sterile water, respectively.
649 Subsequently, all peanut and maize seeds were immersed in sterile water containing
650 10^6 spores/mL of all strains at 29°C in the dark for 60 min. After the conidia adhesion,
651 the seeds were cultured at 29°C for 6 days in the dark [64].

652 **Quantitative RT-PCR**

653 For the real-time quantitative PCR (qPCR) assays, the *A. flavus* strains were
654 cultivated in PDA medium at 29°C for 3 days in the dark. Total RNA was extracted
655 from the mycelia of all strains, and cDNA was synthesized with the First Strand
656 cDNA Synthesis Kit, and then the cDNA was used as the template for qRT-PCR

657 analysis with SYBR Green qPCR mix. The relative transcript level of each gene was
658 calculated by the $2^{-\Delta\Delta CT}$method [66].

659 **Western blot analysis**

660 To extract the total protein, the mycelia of each strain were cultivated in YES
661 liquid medium for 48 h, then the sample was grinded under liquid nitrogen to a fine
662 powder and transferred to a 1.5 mL microcentrifuge tube added with RIPA lysis buffer
663 and 1 mM PMSF protease inhibitor. Proteins were separated by 12% SDS-PAGE and
664 transferred onto a polyvinylidene fluoride (PVDF) membrane. Phosphorylation levels
665 of Hog1 and Slt2 were detected by Phospho-p38 MAPK antibody (Cell Signaling
666 Technology, Boston, MA, USA) and Phospho-p44/42 MAPK (Erk 1/2) antibody (Cell
667 signaling Technology, MA, USA), respectively. The experiment was conducted three
668 times independently.

669 **Statistical analysis**

670 All data were measured with means ± standard deviation (SD) of three biological
671 replicates. Graph Pad Prism 7 software was used for conducting statistical and
672 significance analysis, and p-values < 0.05 was represented statistical significance.
673 Student's *t*-test was used to compare the two means for differences, whereas Tukey's
674 multiple comparisons were used for testing multiple comparisons.

675 **Acknowledgments**

676 The authors also thank Professor Zhenhong Zhuang, Jun Yuan, Yu Wang, Kunzhi
677 Jia, Xiuna Wang, and Xinyi Nie for their help in the experiments. This work was

supported by the National Natural Science Foundation of China (Grant No. 31972214).

Author contributions

Guoqi Li and Xiaohong Cao designed the experiments. Guoqi Li, Xiaohong Cao, and Qianhua Zeng performed the experiments. Guoqi Li, Xiaohong Cao, and Shihua Wang analyzed the data. Guoqi Li, Elisabeth Tumukunde, and Shihua Wang wrote the manuscript. The manuscript was discussed and revised by all the authors.

References

[1] Klich MA. *Aspergillus flavus*: the major producer of aflatoxin. Mol Plant Pathol. 2007; 8(6): 713-22.

[2] Hedayati MT, Pasqualotto AC, Warn PA, et al. *Aspergillus flavus*: human pathogen, allergen and mycotoxin producer. Microbiology (Reading). 2007; 153(Pt 6): 1677-1692.

[3] Khan R, Ghazali FM, Mahyudin NA, et al. Biocontrol of aflatoxins using non-aflatoxigenic *Aspergillus flavus*: a literature review. J Fungi (Basel). 2021; 7(5): 381.

[4] Yabe K, Nakajima H. Enzyme reactions and genes in aflatoxin biosynthesis. Appl Microbiol Biotechnol. 2004; 64(6): 745-55.

[5] Wullschleger S, Loewith R, Hall MN. TOR signaling in growth and metabolism. Cell. 2006; 124(3): 471-84.

[6] De Virgilio C, Loewith R. The TOR signalling network from yeast to man. Int J

699 Biochem Cell Biol. 2006; 38(9): 1476-1481.

700 [7] Loewith R, Jacinto E, Wullschleger S, et al. Two TOR complexes, only one of
701 which is rapamycin sensitive, have distinct roles in cell growth control. Mol Cell.
702 2002; 10(3): 457-68.

703 [8] Beauchamp EM, Platanias LC. The evolution of the TOR pathway and its role in
704 cancer. Oncogene. 2013 Aug 22; 32(34): 3923-32.

705 [9] Fu L, Liu Y, Qin G, et al. The TOR-EIN2 axis mediates nuclear signalling to
706 modulate plant growth. Nature. 2021; 591(7849): 288-292.

707 [10] Teichert S, Wottawa M, Schönig B, et al. Role of the *Fusarium fujikuroi* TOR
708 kinase in nitrogen regulation and secondary metabolism. Eukaryot Cell. 2006;
709 5(10): 1807-1819.

710 [11] Crespo JL, Hall MN. Elucidating TOR signaling and rapamycin action: lessons
711 from *Saccharomyces cerevisiae*. Microbiol Mol Biol Rev. 2002; 66(4): 579-591.

712 [12] Rohde JR, Bastidas R, Puria R, et al. Nutritional control via Tor signaling in
713 *Saccharomyces cerevisiae*. Curr Opin Microbiol. 2008; 11(2): 153-60.

714 [13] Ishiguro J, Shibahara K, Ueda Y, et al. Fission yeast TOR signaling is essential
715 for the down-regulation of a hyperactivated stress-response MAP kinase under
716 salt stress. Mol Genet Genomics. 2013; 288(1-2): 63-75.

717 [14] Otsubo Y, Yamamato M. TOR signaling in fission yeast. Crit Rev Biochem Mol
718 Biol. 2008; 43(4): 277-83.

719 [15] Petersen J. TOR signalling regulates mitotic commitment through stress-activated
720 MAPK and Polo kinase in response to nutrient stress. Biochem Soc Trans. 2009;

721 37(Pt1): 273-7.

722 [16] Bastidas RJ, Heitman J, Cardenas ME. The protein kinase Tor1 regulates adhesin
723 gene expression in *Candida albicans*. PLoS Pathog. 2009; 5(2): e1000294.

724 [17] Liu NN, Flanagan PR, Zeng J, et al. Phosphate is the third nutrient monitored by
725 TOR in *Candida albicans* and provides a target for fungal-specific indirect TOR
726 inhibition. Proc Natl Acad Sci U S A. 2017; 114(24): 6346-6351.

727 [18] Hu K, Guo S, Yan G, et al. Ubiquitin regulates TORC1 in yeast *Saccharomyces*
728 *cerevisiae*. Mol Microbiol. 2016; 100(2): 303-314.

729 [19] Wang H, Wang X, Jiang Y. Interaction with Tap42 is required for the essential
730 function of Sit4 and type 2A phosphatases. Mol Biol Cell. 2003; 14(11): 4342-51.

731 [20] Yan G, Shen X, Jiang Y. Rapamycin activates Tap42-associated phosphatases by
732 abrogating their association with Tor complex 1. EMBO J. 2006; 25(15):
733 3546-55.

734 [21] Tate JJ, Tolley EA, Cooper TG. Sit4 and PP2A Dephosphorylate Nitrogen
735 Catabolite Repression-Sensitive Gln3 When TorC1 Is Up- as Well as
736 Downregulated. Genetics. 2019; 212(4): 1205-1225.

737 [22] Urban J, Soulard A, Huber A, et al. Sch9 is a major target of TORC1 in
738 *Saccharomyces cerevisiae*. Mol Cell. 2007; 26(5): 663-74.

739 [23] Yu F, Gu Q, Yun Y, et al. The TOR signaling pathway regulates vegetative
740 development and virulence in *Fusarium graminearum*. New Phytol. 2014; 203(1):
741 219-32.

742 [24] Liu N, Yun Y, Yin Y, et al. Lipid droplet biogenesis regulated by the

743 FgNem1/Spo7-FgPah1 phosphatase cascade plays critical roles in fungal
744 development and virulence in *Fusarium graminearum*. New Phytol. 2019; 223(1):
745 412-429.
746 [25] Sun G, Elowsky C, Li G, et al. TOR-autophagy branch signaling via Imp1
747 dictates plant-microbe biotrophic interface longevity. PLoS Genet. 2018; 14(11):
748 e1007814.
749 [26] Nguyen DV, Roret T, Fernandez-Gonzalez A, et al. Target of rapamycin pathway
750 in the white-rot fungus *Phanerochaete chrysosporium*. PLoS One. 2020; 15(2):
751 e0224776.
752 [27] Dementhon K, Paoletti M, Pinan-Lucarré B, et al. Rapamycin mimics the
753 incompatibility reaction in the fungus *Podospora anserina*. Eukaryot Cell. 2003;
754 2(2): 238-46.
755 [28] Fitzgibbon GJ, Morozov IY, Jones MG, et al. Genetic analysis of the TOR
756 pathway in *Aspergillus nidulans*. Eukaryot Cell. 2005; 4(9): 1595-8.
757 [29] Alves de Castro P, Dos Reis TF, et al. The *Aspergillus fumigatus* $SchA^{SCH9}$ kinase
758 modulates $SakA^{HOG1}$ MAP kinase activity and it is essential for virulence. Mol
759 Microbiol. 2016; 102(4): 642-671.
760 [30] Baldin C, Valiante V, Krüger T, et al. Comparative proteomics of a tor inducible
761 *Aspergillus fumigatus* mutant reveals involvement of the Tor kinase in iron
762 regulation. Proteomics. 2015; 15(13): 2230-43.
763 [31] Teichert S, Wottawa M, Schönig B, et al. Role of the *Fusarium fujikuroi* TOR
764 kinase in nitrogen regulation and secondary metabolism. Eukaryot Cell. 2006;

765 5(10): 1807-19.

766 [32] Meléndez HG, Billon-Grand G, Fèvre M, et al. Role of the *Botrytis cinerea*
767 FKBP12 ortholog in pathogenic development and in sulfur regulation. Fungal
768 Genet Biol. 2009; 46(4): 308-20.

769 [33] López-Berges MS, Rispail N, Prados-Rosales RC, et al. A nitrogen response
770 pathway regulates virulence functions in *Fusarium oxysporum* via the protein
771 kinase TOR and the bZIP protein MeaB. Plant Cell. 2010; 22(7): 2459-75.

772 [34] Bastidas RJ, Shertz CA, Lee SC, et al. Rapamycin exerts antifungal activity *in*
773 *vitro* and *in vivo* against *Mucor circinelloides* via FKBP12-dependent inhibition
774 of Tor. Eukaryot Cell. 2012; 11(3): 270-81.

775 [35] Madrid, M, Vázquez-Marín, B, Franco, A, et al. Multiple crosstalk between TOR
776 and the cell integrity MAPK signaling pathway in fission yeast. Sci Rep. 2016
777 Nov 23; 6: 37515.

778 [36] Torres J, Di Como CJ, Herrero E, et al. Regulation of the cell integrity pathway
779 by rapamycin-sensitive TOR function in budding yeast. J Biol Chem. 2002 Nov 8;
780 277(45): 43495-504.

781 [37] Chen DD, Shi L, Yue SN, et al. The Slt2-MAPK pathway is involved in the
782 mechanism by which target of rapamycin regulates cell wall components in
783 *Ganoderma lucidum*. Fungal Genet Biol. 2019; 123: 70-77.

784 [38] Gu Q, Zhang C, Yu F, et al. Protein kinase FgSch9 serves as a mediator of the
785 target of rapamycin and high osmolarity glycerol pathways and regulates multiple
786 stress responses and secondary metabolism in *Fusarium graminearum*. Environ

787 Microbiol. 2015; 17(8): 2661-76.

788 [39] Qian B, Liu X, Jia J, et al. MoPpe1 partners with MoSap1 to mediate TOR and
789 cell wall integrity signalling in growth and pathogenicity of the rice blast fungus
790 *Magnaporthe oryzae*. Environ Microbiol. 2018; 20(11): 3964-3979.

791 [40] Qian B, Liu X, Ye Z, et al. Phosphatase-associated protein MoTip41 interacts
792 with the phosphatase MoPpe1 to mediate crosstalk between TOR and cell wall
793 integrity signalling during infection by the rice blast fungus *Magnaporthe oryzae*.
794 Environ Microbiol. 2021; 23(2): 791-809.

795 [41] Tong M, Jiang Y. FK506-Binding Proteins and Their Diverse Functions. Curr Mol
796 Pharmacol. 2015; 9(1): 48-65.

797 [42] Heitman J, Movva NR, Hall MN. Targets for cell cycle arrest by the
798 immunosuppressant rapamycin in yeast. Science. 1991; 253(5022): 905-9.

799 [43] Ren S, Yang M, Yue Y, et al. Lysine Succinylation Contributes to Aflatoxin
800 Production and Pathogenicity in *Aspergillus flavus*. Mol Cell Proteomics. 2018;
801 17(3): 457-471.

802 [44] Weisman R. Target of Rapamycin (TOR) Regulates Growth in Response to
803 Nutritional Signals. Microbiol Spectr. 2016 Oct; 4(5).

804 [45] Loewith R, Hall MN. Target of rapamycin (TOR) in nutrient signaling and
805 growth control. Genetics. 2011 Dec; 189(4): 1177-201.

806 [46] Pascual-Ahuir A, Proft M. The Sch9 kinase is a chromatin-associated
807 transcriptional activator of osmostress-responsive genes. EMBO J. 2007; 26(13):
808 3098-108.

809 [47] Düvel K, Broach JR. The role of phosphatases in TOR signaling in yeast. Curr
810 Top Microbiol Immunol. 2004; 279: 19-38.
811 [48] Jacinto E, Guo B, Arndt KT, et al. TIP41 interacts with TAP42 and negatively
812 regulates the TOR signaling pathway. Mol Cell. 2001; 8(5): 1017-26.
813 [49] Sánchez-Álvarez M, Del Pozo MÁ, Bosch M, et al. Insights into the biogenesis
814 and emerging functions of lipid droplets from unbiased molecular profiling
815 approaches. Front Cell Dev Biol. 2022 Jun 8; 10: 901321.
816 [50] Gizachew D, Chang CH, Szonyi B, et al. Aflatoxin B1 (AFB_1) production by
817 *Aspergillus flavus* and *Aspergillus parasiticus* on ground Nyjer seeds: The effect
818 of water activity and temperature. Int J Food Microbiol. 2019; 296: 8-13.
819 [51] Cruz MC, Goldstein AL, Blankenship J, et al. Rapamycin and less
820 immunosuppressive analogs are toxic to *Candida albicans* and *Cryptococcus*
821 *neoformans* via FKBP12-dependent inhibition of TOR. Antimicrob Agents
822 Chemother. 2001; 45(11): 3162-70.
823 [52] Galat A. Functional diversity and pharmacological profiles of the FKBPs and
824 their complexes with small natural ligands. Cell Mol Life Sci. 2013; 70(18):
825 3243-75.
826 [53] Kasahara K. Physiological function of FKBP12, a primary target of
827 rapamycin/FK506: a newly identified role in transcription of ribosomal protein
828 genes in yeast. Curr Genet. 2021 Jun; 67(3): 383-388.
829 [54] Li Y, Ren H, Zhao Y, et al. Characterization of three FK506-binding proteins in
830 the entomopathogenic fungus *Beauveria bassiana*. J Invertebr Pathol. 2020; 171:

831 107334.

832 [55] Xiong Y, Sheen J. The role of target of rapamycin signaling networks in plant
833 growth and metabolism. Plant Physiol. 2014; 164(2): 499-512.

834 [56] Adami A, García-Alvarez B, Arias-Palomo E, et al. Structure of TOR and its
835 complex with KOG1. Mol Cell. 2007; 27(3): 509-16.

836 [57] Ma YC, Dai LL, Qiu BB, et al. TOR functions as a molecular switch connecting
837 an iron cue with host innate defense against bacterial infection. PLoS Genet. 2021;
838 17(3): e1009383.

839 [58] Baldin C, Valiante V, Krüger T, et al. Comparative proteomics of a tor inducible
840 *Aspergillus fumigatus* mutant reveals involvement of the Tor kinase in iron
841 regulation. Proteomics. 2015; 15(13): 2230-43.

842 [59] Pascual-Ahuir A, Proft M. The Sch9 kinase is a chromatin-associated
843 transcriptional activator of osmostress-responsive genes. EMBO J. 2007; 26(13):
844 3098-108.

845 [60] Fenyvuesvolgyi C, Elder RT, Benko Z, et al. Fission yeast homologue of
846 Tip41-like proteins regulates type 2A phosphatases and responses to nitrogen
847 sources. Biochim Biophys Acta. 2005; 1746(2): 155-62.

848 [61] Nakashima A, Tanimura-Ito K, Oshiro N, et al. A positive role of mammalian
849 Tip41-like protein, TIPRL, in the amino-acid dependent mTORC1-signaling
850 pathway through interaction with PP2A. FEBS Lett. 2013; 587(18): 2924-9.

851 [62] Han Q, Pan C, Wang Y, et al. PP2A-like protein phosphatase (Sit4) regulatory
852 subunits, Sap155 and Sap190, regulate *Candida albicans*' cell growth,

853 morphogenesis, and virulence. Front Microbiol. 2019 Dec 20; 10: 2943.

854 [63] Tan L, Chen H, Yu S, et al. A SOE-PCR method of introducing multiple
855 mutations into Mycoplasma gallisepticum neuraminidase. J Microbiol Methods.
856 2013; 94(2): 117-120.

857 [64] Nie X, Yu S, Qiu M, et al. *Aspergillus flavus* SUMO contributes to fungal
858 virulence and toxin attributes. J Agric Food Chem. 2016 Sep 7; 64(35): 6772-82.

859 [65] Wang Y, Wang S, Nie X, et al. Molecular and structural basis of nucleoside
860 diphosphate kinase-mediated regulation of spore and sclerotia development in the
861 fungus *Aspergillus flavus*. J Biol Chem. 2019 Aug 16; 294(33): 12415-12431.

862 [66] Livak KJ, Schmittgen TD. Analysis of relative gene expression data using
863 real-time quantitative PCR and the $2^{-\Delta\Delta CT}$ method. Methods. 2001; 25(4):
864 402–408.

865

866

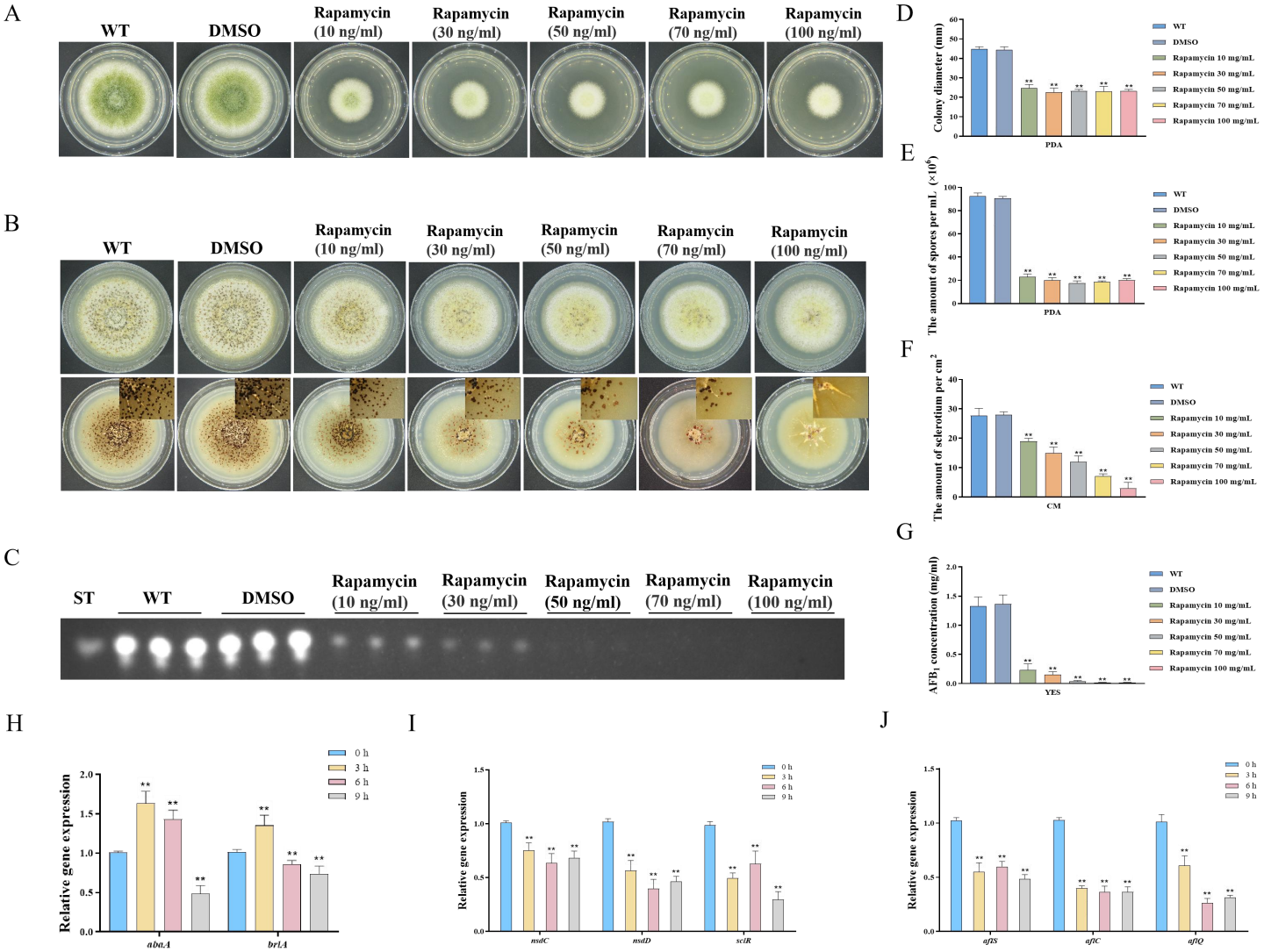
A
WT
DMSO
Rapamycin (10 ng/ml)
Rapamycin (30 ng/ml)
Rapamycin (50 ng/ml)
Rapamycin (70 ng/ml)
Rapamycin (100 ng/ml)
B
C
ST
D
Colony diameter (mm)
PDA
E
The amount of spores per mL (×10^6)
F
The amount of sclerotium per cm^2
CM
G
AFB1 concentration (mg/ml)
YES
Rapamycin 10 mg/mL
Rapamycin 30 mg/mL
Rapamycin 50 mg/mL
Rapamycin 70 mg/mL
Rapamycin 100 mg/mL
H
Relative gene expression
0 h
3 h
6 h
9 h
abaA
brlA
I
nsdC
nsdD
sclR
J
aflS
aflC
aflQ

Fig. 1 Impacts of rapamycin on the growth, sporulation, sclerotia formation,and aflatoxin production of *Aspergillus flavus*.

(A) Colony morphology of the WT strain cultured on PDA medium amended with different concentrations of rapamycin at 37°C for 5 days.

(B) Colony phenotype of the WT strain grown on CM medium amended with different concentrations of rapamycin at 37°C for 7 days.

(C) TLC assay of AFB_1 production by the WT strain cultured in YES liquid media amended with different concentrations of rapamycin at 29°C for 6 days.

(D) Statistical analysis of the colony diameter by the WT strain treated with different concentrations of rapamycin described in (A).

(E) Conidial quantification of the WT strain treated with different concentrations of rapamycin as mentioned in (A).

(F) Quantitative analysis of sclerotium formation by the WT strain treated with different concentrations of rapamycin described in (B).

(G) Relative quantification of AFB_1 production by the WT strain treated with different concentrations of rapamycin as mentioned in (C)

(H) Relative expression levels of conidia-related genes in WT strain treated with 100 ng/mL rapamycin after 3, 6, 9 h.

(I) Relative expression levels of sclerotia-related genes in WT strain treated with 100 ng/mL rapamycin after 3, 6, 9 h.

(J) Relative expression levels of aflatoxin biosynthesis regulatory and structural genes in WT strain treated with 100 ng/mL rapamycin after 3, 6, 9 h.

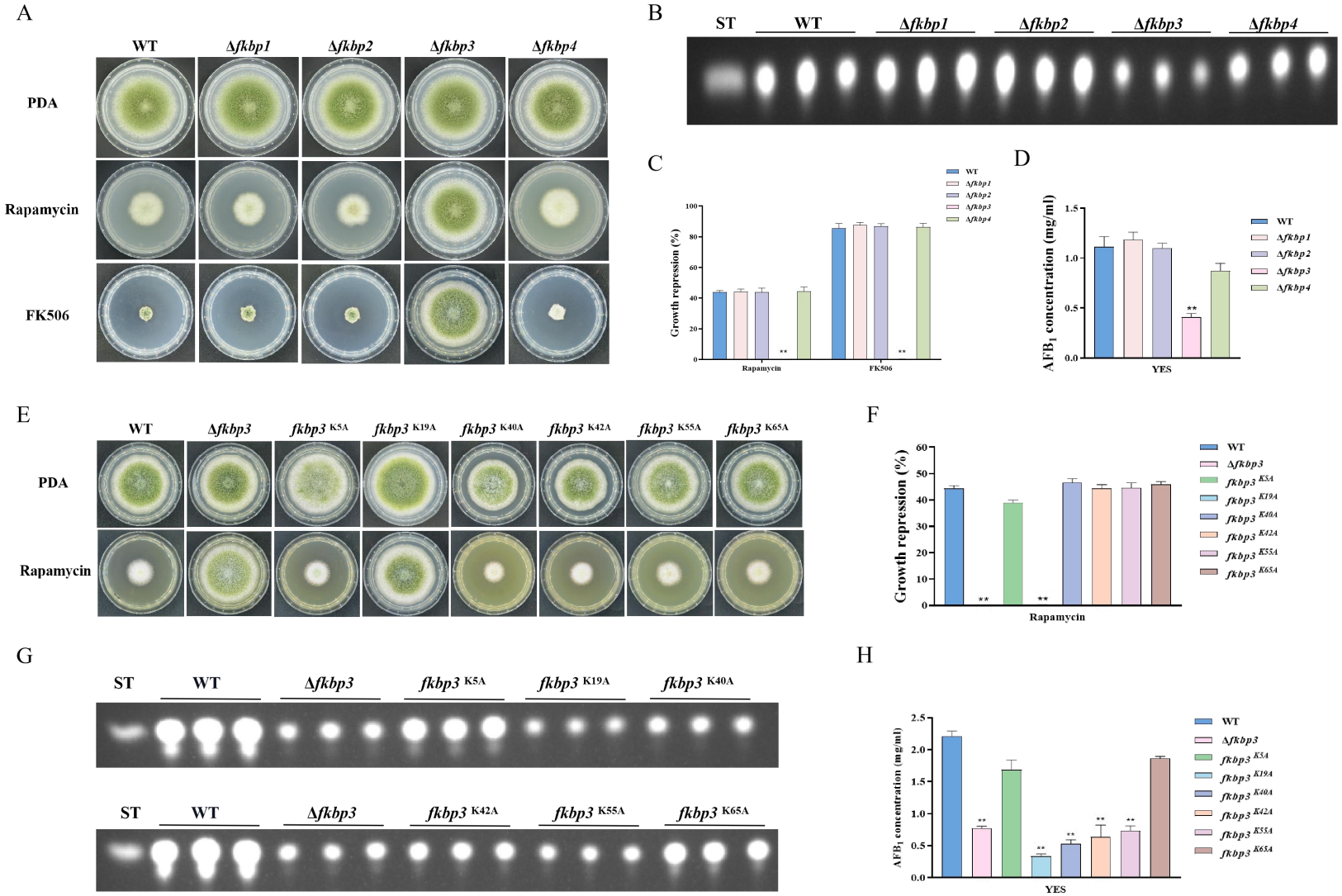
A
WT
Δfkbp1
Δfkbp2
Δfkbp3
Δfkbp4
PDA
Rapamycin
FK506
B
ST
WT
Δfkbp1
Δfkbp2
Δfkbp3
Δfkbp4
C
Growth repression (%)
Rapamycin
FK506
D
AFB1 concentration (mg/ml)
YES
E
WT
Δfkbp3
fkbp3 K5A
fkbp3 K19A
fkbp3 K40A
fkbp3 K42A
fkbp3 K55A
fkbp3 K65A
PDA
Rapamycin
F
Growth repression (%)
Rapamycin
G
ST
WT
Δfkbp3
fkbp3 K5A
fkbp3 K19A
fkbp3 K40A
fkbp3 K42A
fkbp3 K55A
fkbp3 K65A
H
AFB1 concentration (mg/ml)
YES

Fig. 2 Disruption of *fkbp3* significantly increases the resistance of *A. flavus* to rapamycin and FK506.

(A) Phenotype of the WT and all mutant strains (Δ*fkbp1*, Δ*fkbp2*, Δ*fkbp3*, and Δ*fkbp4*) grown on PDA amended with rapamycin and FK506 at 37°C for 5 days.

(B) TLC analysis of AFB_1 production by the WT and all mutant strains (Δ*fkbp1*, Δ*fkbp2*, Δ*fkbp3*, and Δ*fkbp4*) cultured in YES liquid medium at 29°C for 6 days.

(C) The growth inhibition rate of the WT and all mutant strains (Δ*fkbp1*, Δ*fkbp2*, Δ*fkbp3*, and Δ*fkbp4*) under rapamycin and FK506 stress.

(D) AFB_1 quantitative analysis of the WT and all mutant strains (Δ*fkbp1*, Δ*fkbp2*, Δ*fkbp3*, and Δ*fkbp4*) as described in (B).

(E) Phenotype of the WT and all mutant strains (Δ*fkbp3*, K5A, K19A, K40A, K42A, K55A, and K65A) grown on PDA amended with 100 ng/mL rapamycin at 37°C for 5 days.

(F) The growth inhibition rate of the WT and all mutant strains (Δ*fkbp3*, K5A, K19A, K40A, K42A, K55A, and K65A) under rapamycin stress.

(G) TLC assay of AFB_1 production by the WT and all mutant strains (Δ*fkbp3*, K5A, K19A, K40A, K42A, K55A, and K65A) cultured in YES liquid medium at 29°C for 6 days.

(H) Relative quantification of AFB_1 production in the WT and all mutant strains (Δ*fkbp3*, K5A, K19A, K40A, K42A, K55A, and K65A) as mentioned in (G).

A

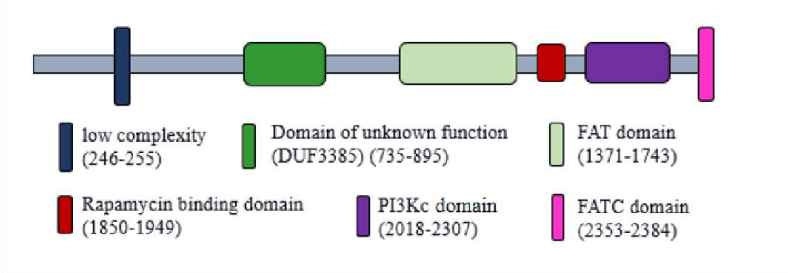
low complexity
(246-255)
Domain of unknown function
(DUF3385) (735-895)
FAT domain
(1371-1743)
Rapamycin binding domain
(1850-1949)
PI3Kc domain
(2018-2307)
FATC domain
(2353-2384)

B

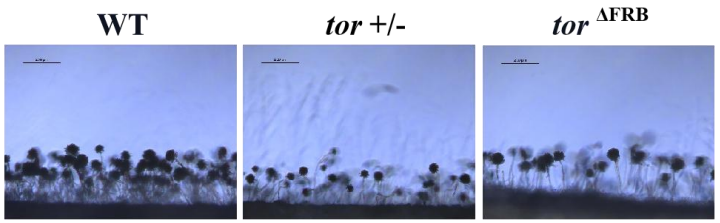
WT
tor +/-
tor ΔFRB

C

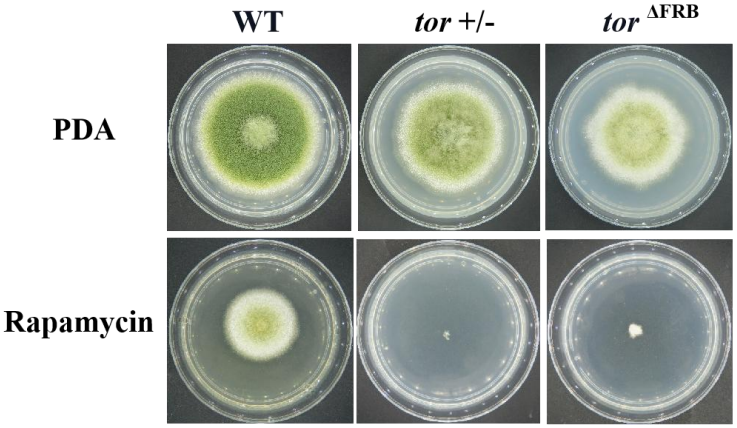
WT
tor +/-
tor ΔFRB
PDA
Rapamycin

D

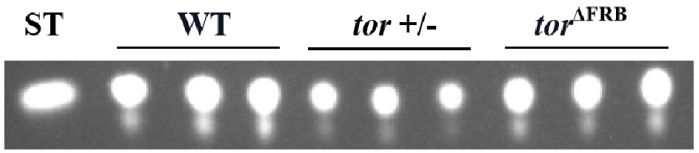
ST
WT
tor +/-
tor ΔFRB

E

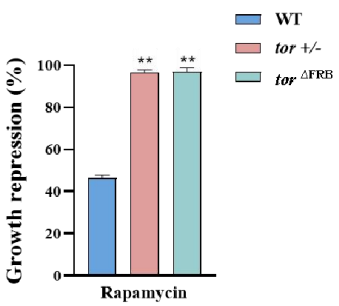
WT
tor +/-
tor ΔFRB
Growth repression (%)
100
80
60
40
20
0
**
**
Rapamycin

F

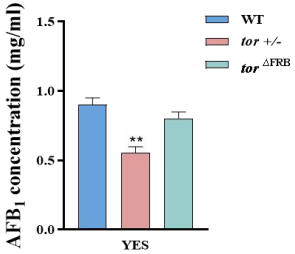
WT
tor +/-
tor ΔFRB
AFB1 concentration (mg/ml)
1.5
1.0
0.5
0.0
**
YES

Fig. 3 The Tor kinase plays a vital role in *A. flavus*.

(A) The structure diagram of the Tor kinase.

(B) Morphology of conidiophores in the WT, *tor*+/-, and *tor*$^{\Delta FRB}$strains observed by microscope.

(C) Phenotype of the WT, *tor*+/-, and *tor*$^{\Delta FRB}$strains grown on PDA amended with 100 ng/mL rapamycin at 37°C for 5 days.

(D) TLC assay of AFB_1 production by the WT, *tor*+/-, and *tor*$^{\Delta FRB}$strains cultured in YES liquid medium at 29°C for 6 days.

(E) The growth inhibition rate of the WT, *tor*+/-, and *tor*$^{\Delta FRB}$strains under rapamycin stress.

(F) AFB_1 quantitative analysis of the WT, *tor*+/-, and *tor*$^{\Delta FRB}$strains described in (D).

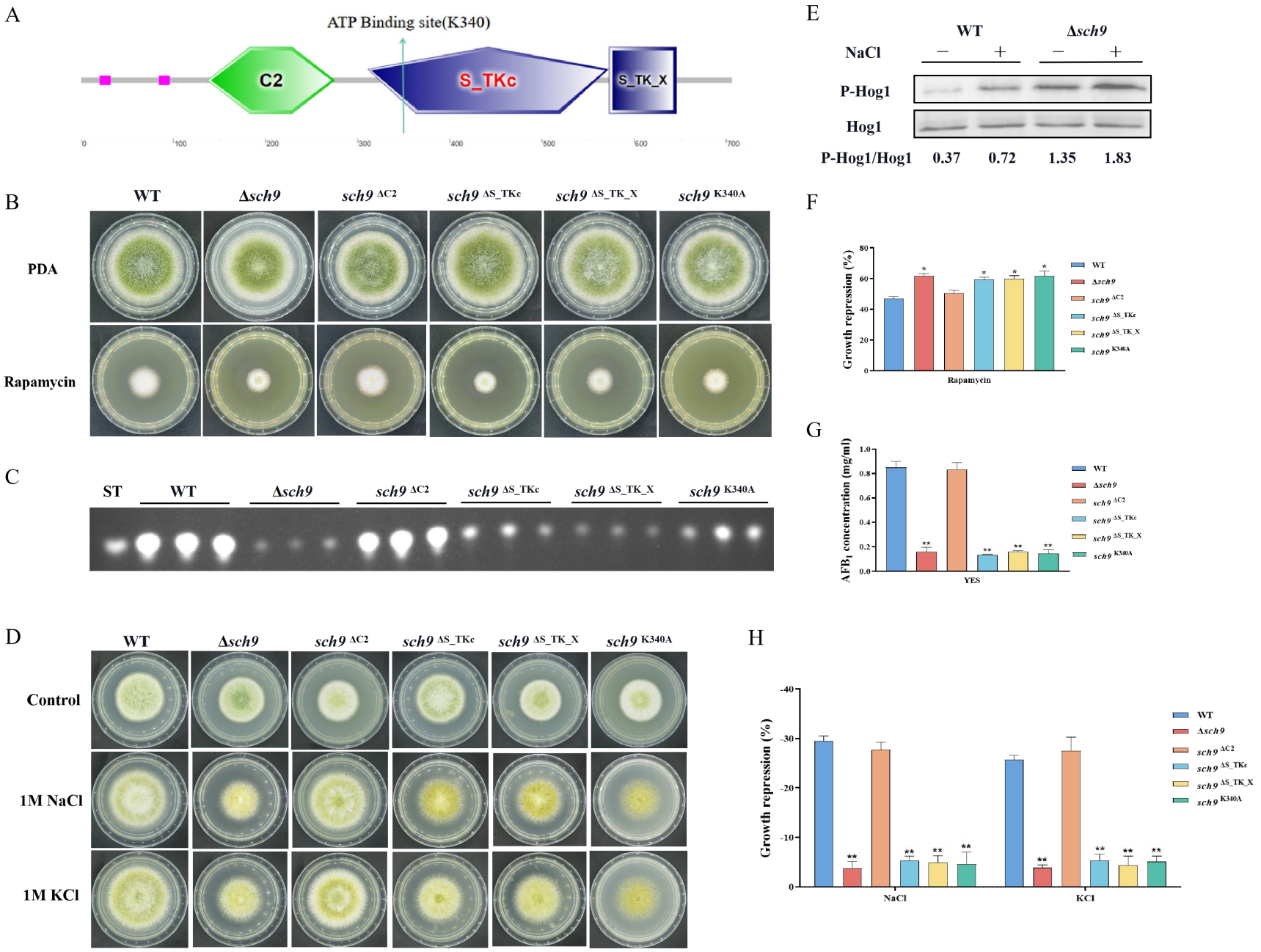
A
ATP Binding site(K340)
C2
S_TKc
S_TK_X
0
100
200
300
400
500
600
700
B
WT
Δsch9
sch9 ΔC2
sch9 ΔS_TKc
sch9 ΔS_TK_X
sch9 K340A
PDA
Rapamycin
C
ST
WT
Δsch9
sch9 ΔC2
sch9 ΔS_TKc
sch9 ΔS_TK_X
sch9 K340A
D
WT
Δsch9
sch9 ΔC2
sch9 ΔS_TKc
sch9 ΔS_TK_X
sch9 K340A
Control
1M NaCl
1M KCl
E
WT
Δsch9
NaCl
−
+
−
+
P-Hog1
Hog1
P-Hog1/Hog1
0.37
0.72
1.35
1.83
F
Growth repression (%)
80
60
40
20
0
Rapamycin
WT
Δsch9
sch9 ΔC2
sch9 ΔS_TKc
sch9 ΔS_TK_X
sch9 K340A
G
AFB1 concentration (mg/ml)
1.0
0.8
0.6
0.4
0.2
0.0
YES
WT
Δsch9
sch9 ΔC2
sch9 ΔS_TKc
sch9 ΔS_TK_X
sch9 K340A
H
Growth repression (%)
-40
-30
-20
-10
0
NaCl
KCl
WT
Δsch9
sch9 ΔC2
sch9 ΔS_TKc
sch9 ΔS_TK_X
sch9 K340A

Fig. 4 The Sch9 kinase participates in aflatoxin biosynthesis and the HOG pathway.

(A) The structure diagram of the Sch9 kinase.

(B) Phenotype of the WT, Δ*sch9*, *sch9*$^{\Delta C2}$, *sch9*$^{\Delta S_TKc}$, *sch9*$^{\Delta S_TK_X}$, and *sch9*^{K340A} strains grown on PDA medium amended with 100 ng/mL rapamycin at 37°C for 5 days.

(C) TLC assay of AFB_1 production from the WT, Δ*sch9*, *sch9*$^{\Delta C2}$, *sch9*$^{\Delta S_TKc}$, *sch9*$^{\Delta S_TK_X}$, and *sch9*^{K340A} strains cultured in YES liquid medium at 29°C for 6 days.

(D) The phenotypes of the WT, Δ*sch9*, *sch9*$^{\Delta C2}$, *sch9*$^{\Delta S_TKc}$, *sch9*$^{\Delta S_TK_X}$, and *sch9*^{K340A}strains on YGT media amended with 1 M NaCl and 1 M KCl for 3 days.

(E) The phosphorylation levels of Hog1 in the WT and Δ*sch9* strains were determined with or without osmotic stress.

(F) The growth inhibition rate of the WT, Δ*sch9*, *sch9*$^{\Delta C2}$, *sch9*$^{\Delta S_TKc}$, *sch9*$^{\Delta S_TK_X}$, and *sch9*^{K340A} strains under rapamycin stress.

(G) Quantitative analysis of AFB_1 as shown in (C).

(H) The growth inhibition rate of the WT, Δ*sch9*, *sch9*$^{\Delta C2}$, *sch9*$^{\Delta S_TKc}$, *sch9*$^{\Delta S_TK_X}$, and *sch9*^{K340A} strains under osmotic stress.

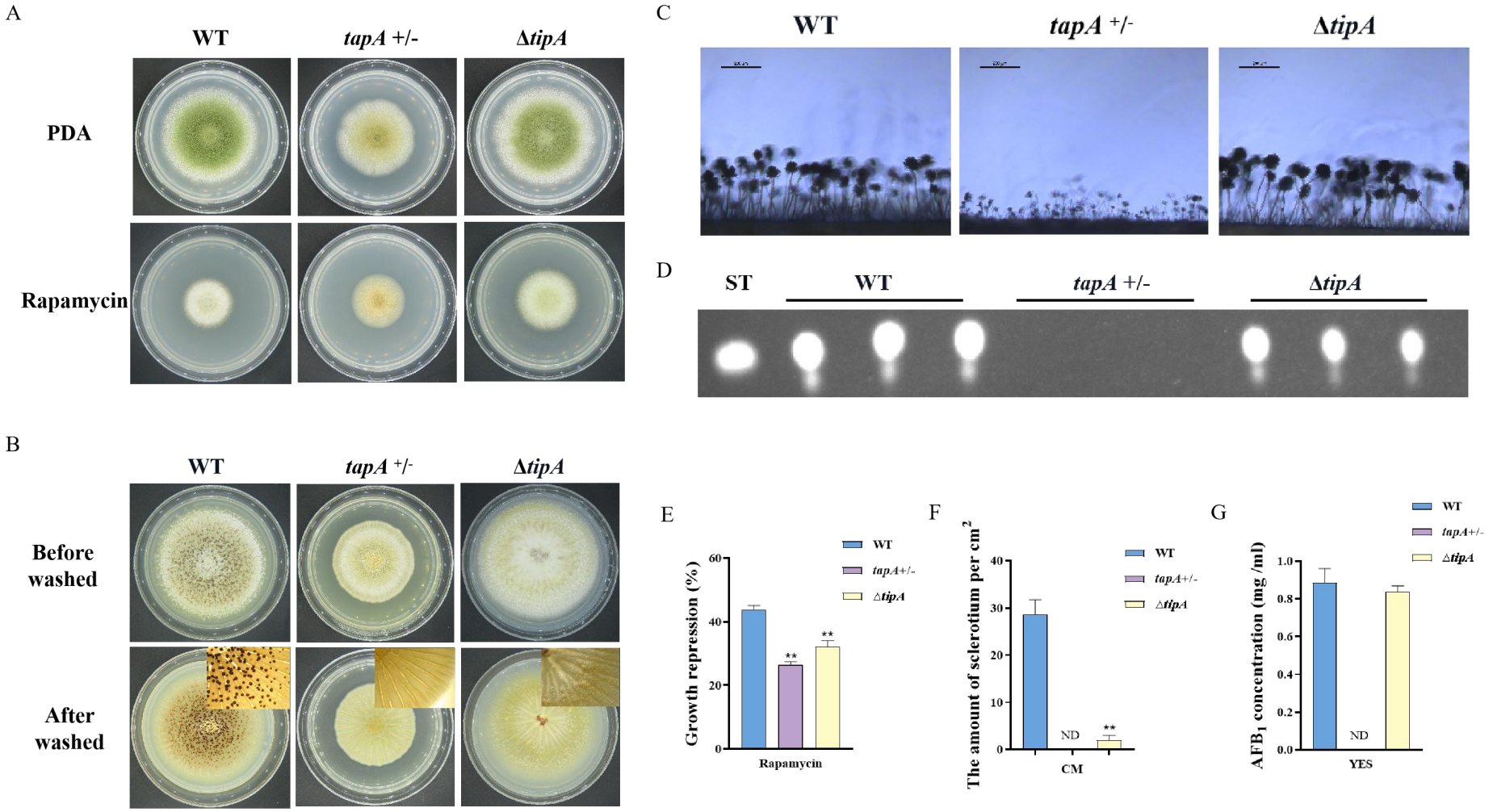
A
WT
tapA +/-
ΔtipA
PDA
Rapamycin
B
WT
tapA +/-
ΔtipA
Before washed
After washed
C
WT
tapA +/-
ΔtipA
D
ST
WT
tapA +/-
ΔtipA
E
Growth repression (%)
60
40
20
0
**
**
Rapamycin
WT
tapA+/-
ΔtipA
F
The amount of sclerotium per cm2
40
30
20
10
0
ND
**
CM
WT
tapA+/-
ΔtipA
G
AFB1 concentration (mg /ml)
1.0
0.8
0.6
0.4
0.2
0.0
ND
YES
WT
tapA+/-
ΔtipA

Fig. 5 TapA and TipA regulate sclerotia formation in *A. flavus.*

(A) Phenotype of the WT, *tapA* +/-, and Δ*tipA* strains grown on PDA amended with 100 ng/mL rapamycin at 37°C for 5 days.

(B) Phenotypic characterization of the WT, *tapA* +/-, and Δ*tipA* strains grown on CM medium at 37°C for 7 days.

(C) Morphology of conidiophores in the WT, *tapA* +/-, and Δ*tipA* strains observed by microscope.

(D) TLC assay of AFB_1 production by the WT, *tapA* +/-, and Δ*tipA* strains cultured in YES liquid medium at 29°C for 6 days.

(E) The growth inhibition rate of the WT, *tapA* +/-, and Δ*tipA* strains under rapamycin stress.

(F) Amount of sclerotia produced by the WT, *tapA* +/-, and Δ*tipA* strains.

(G) AFB_1 quantitative analysis of the WT, *tapA* +/-, and Δ*tipA* strains described in (D).

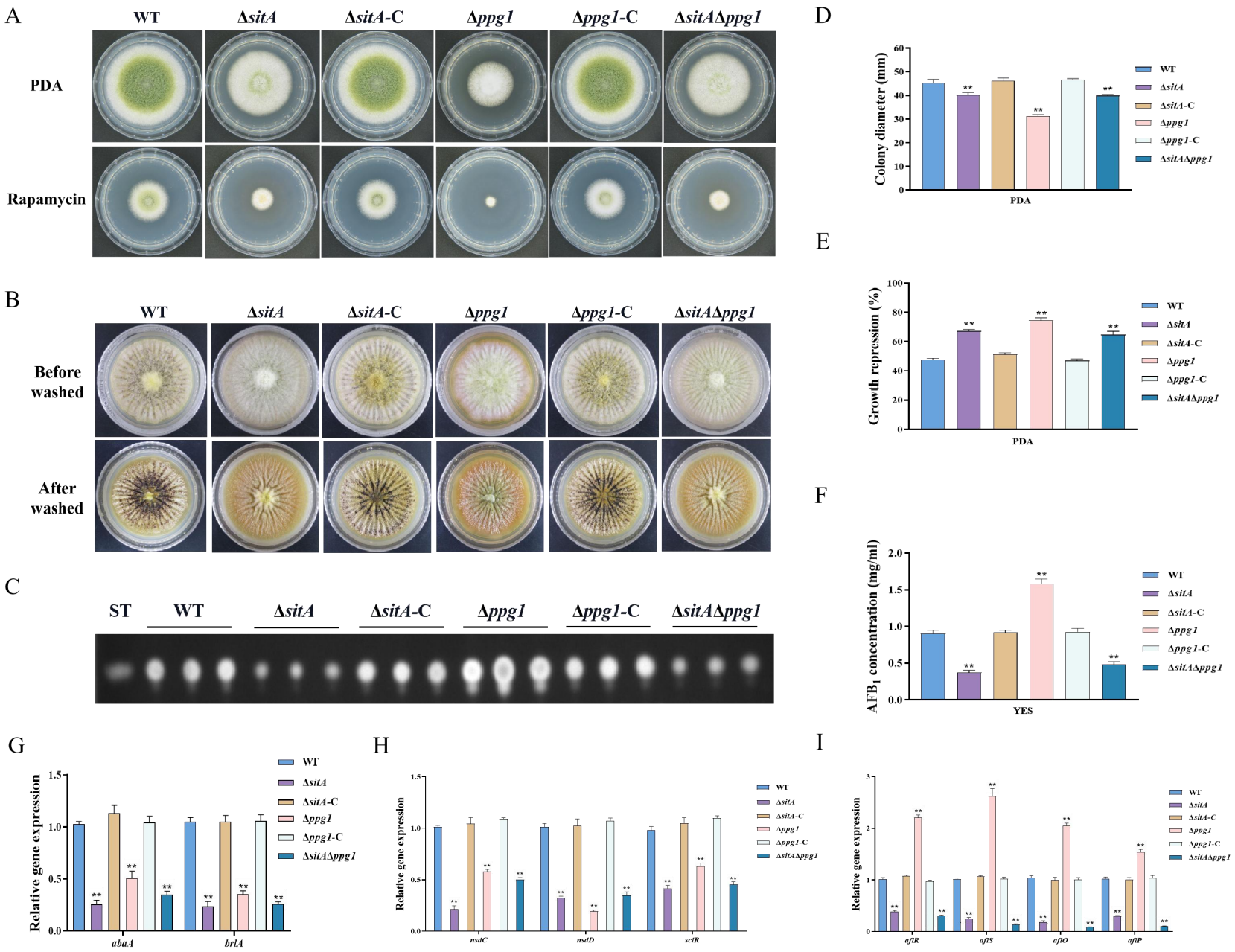
A
WT
ΔsitA
ΔsitA-C
Δppg1
Δppg1-C
ΔsitAΔppg1
PDA
Rapamycin
B
Before washed
After washed
C
ST
D
Colony diameter (mm)
PDA
E
Growth repression (%)
F
AFB1 concentration (mg/ml)
YES
G
Relative gene expression
abaA
brlA
H
nsdC
nsdD
sclR
I
aflR
aflS
aflO
aflP

Fig. 6 The impact of the phosphatases SitA and Ppg1 on the growth, conidiation, and aflatoxin biosynthesis in *A. flavus*.

(A) Colony morphology of the WT, single knockout, and double knockout strains cultured on PDA medium amended with 100 ng/mL rapamycin at 37°C for 5 days.

(B) Colony morphology of the WT, single knockout, and double knockout strains cultured on WKM medium at 37°C for 7 days.

(C) TLC analysis of AFB_1 production from the WT, single knockout, and double knockout strains cultured in YES liquid medium at 29°C for 6 days.

(D) Growth diameter of the WT, single knockout, and double knockout strains on PDA media.

(E) The growth inhibition rate of the WT, single knockout, and double knockout strains under rapamycin stress.

(F) AFB_1 quantitative analysis of the WT, single knockout, and double knockout strains.

(G) Relative expression levels of conidia synthesis genes in the WT, single knockout, and double knockout strains.

(H) Relative expression levels of sclerotia synthesis genes in the WT, single knockout, and double knockout strains.

(I) Relative expression levels of aflatoxin biosynthesis genes in the WT, single knockout, and double knockout strains.

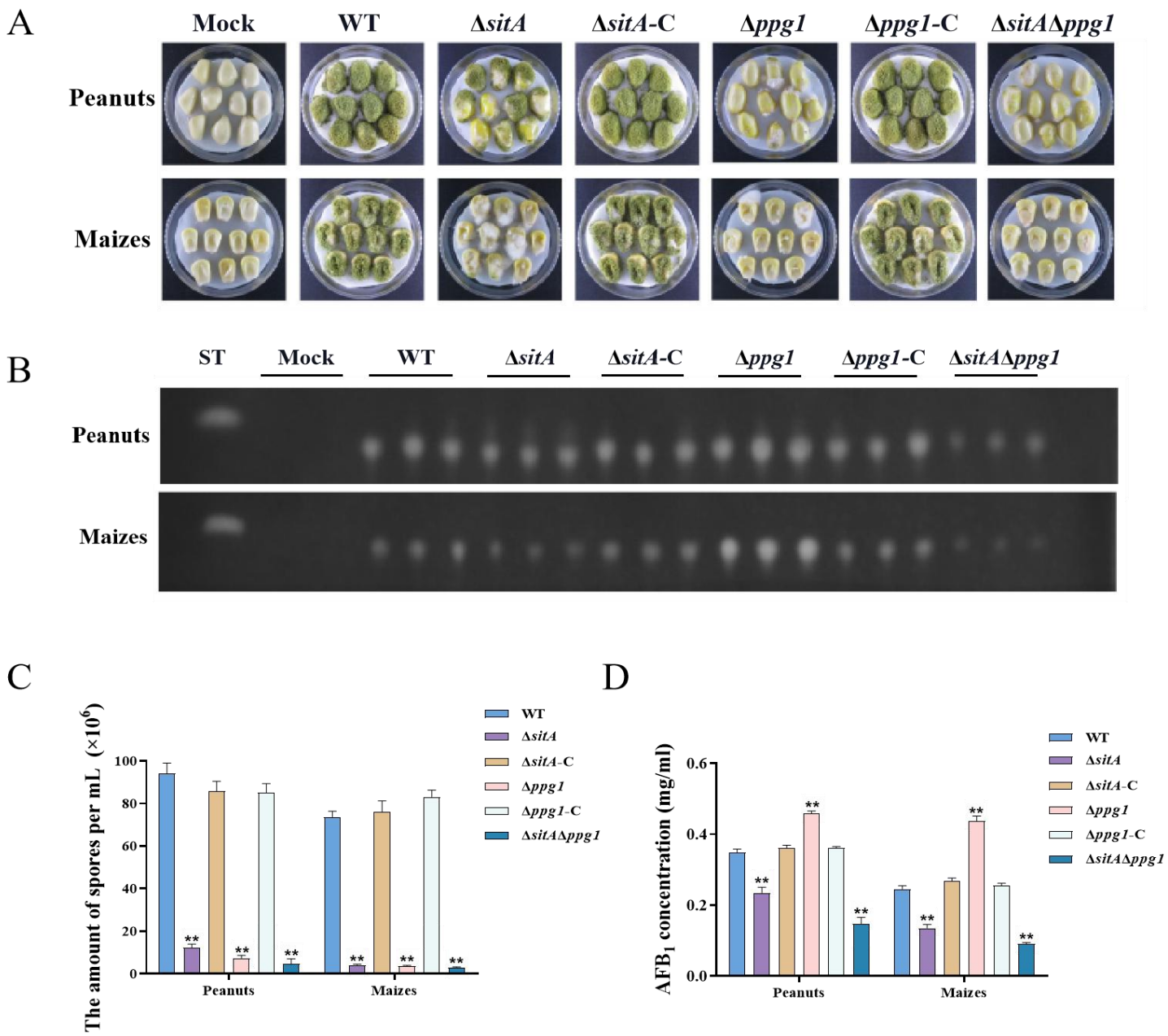
A
Mock
WT
ΔsitA
ΔsitA-C
Δppg1
Δppg1-C
ΔsitAΔppg1
Peanuts
Maizes
B
ST
Mock
WT
ΔsitA
ΔsitA-C
Δppg1
Δppg1-C
ΔsitAΔppg1
Peanuts
Maizes
C
The amount of spores per mL (×10^6)
100
80
60
40
20
0
Peanuts
Maizes
WT
ΔsitA
ΔsitA-C
Δppg1
Δppg1-C
ΔsitAΔppg1
D
AFB1 concentration (mg/ml)
0.6
0.4
0.2
0.0
Peanuts
Maizes
WT
ΔsitA
ΔsitA-C
Δppg1
Δppg1-C
ΔsitAΔppg1

Fig. 7 Pathogenicity analysis of the phosphatase SitA and Ppg1 in *A. flavus*.

(A) Phenotypes of peanut and maize infected by the WT, single knockout, and double knockout strains.

(B) TLC was used to detect the AFB_1 from peanut and maize infected by the WT, single knockout, and double knockout strains.

(C) Quantitative analysis of conidia production from peanut and maize infected by the WT, single knockout, and double knockout strains.

(D) Quantitative analysis of AFB_1 from peanut and maize infected by the WT, single knockout, and double knockout strains.

A

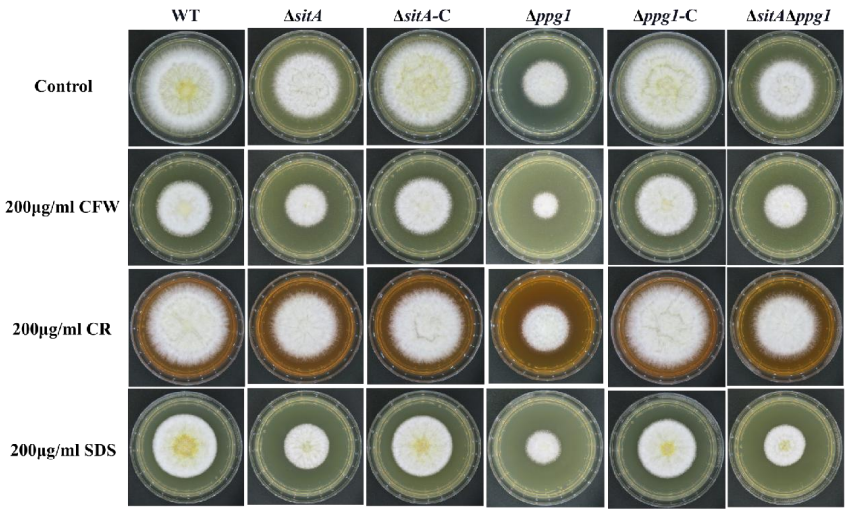
WT
ΔsitA
ΔsitA-C
Δppg1
Δppg1-C
ΔsitAΔppg1
Control
200μg/ml CFW
200μg/ml CR
200μg/ml SDS

B

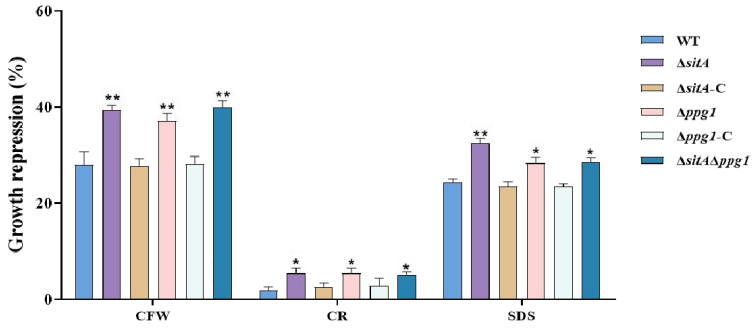
Growth repression (%)
60
40
20
0
CFW
CR
SDS
WT
ΔsitA
ΔsitA-C
Δppg1
Δppg1-C
ΔsitAΔppg1

C

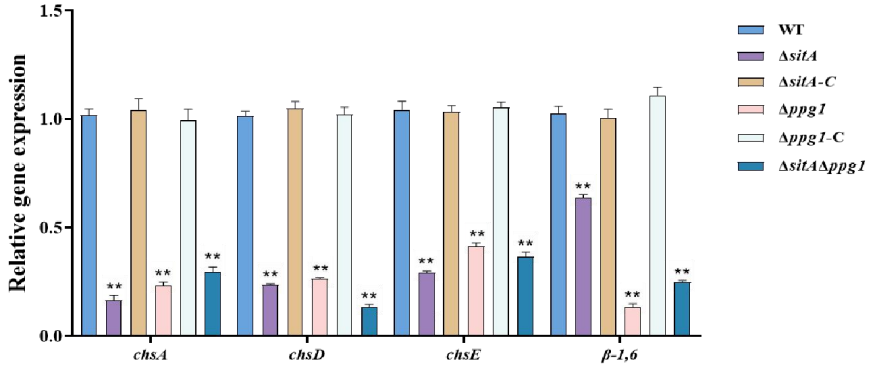
Relative gene expression
1.5
1.0
0.5
0.0
chsA
chsD
chsE
β-1,6
WT
ΔsitA
ΔsitA-C
Δppg1
Δppg1-C
ΔsitAΔppg1

D

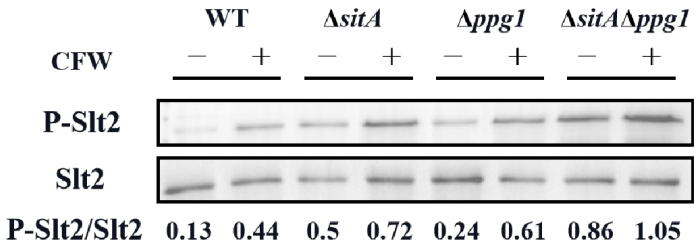
WT
ΔsitA
Δppg1
ΔsitAΔppg1
CFW
− + − + − + − +
P-Slt2
Slt2
P-Slt2/Slt2 0.13 0.44 0.5 0.72 0.24 0.61 0.86 1.05

Fig. 8 Sensitivity of phosphatase SitA and Ppg1 to cell wall damaging agents in *A. flavus*.

(A) Morphology of the WT, single knockout, and double knockout strains grown on YES media supplemented with 200 μg/mL CR, 200 μg/mL CFW, or 100 μg/mL SDS at 37°C for 5 days.

(B) The growth inhibition rate of the WT, single knockout, and double knockout strains under cell wall and cell membrane stress.

(C) Relative expression levels of cell wall synthesis genes (*chsA*, *chsD*, *chsE* and *β-1,6*) in the WT, single knockout, and double knockout strains.

(D) The phosphorylation level of Slt2 in the WT, single knockout, and double knockout strains was detected with or without cell wall stress.

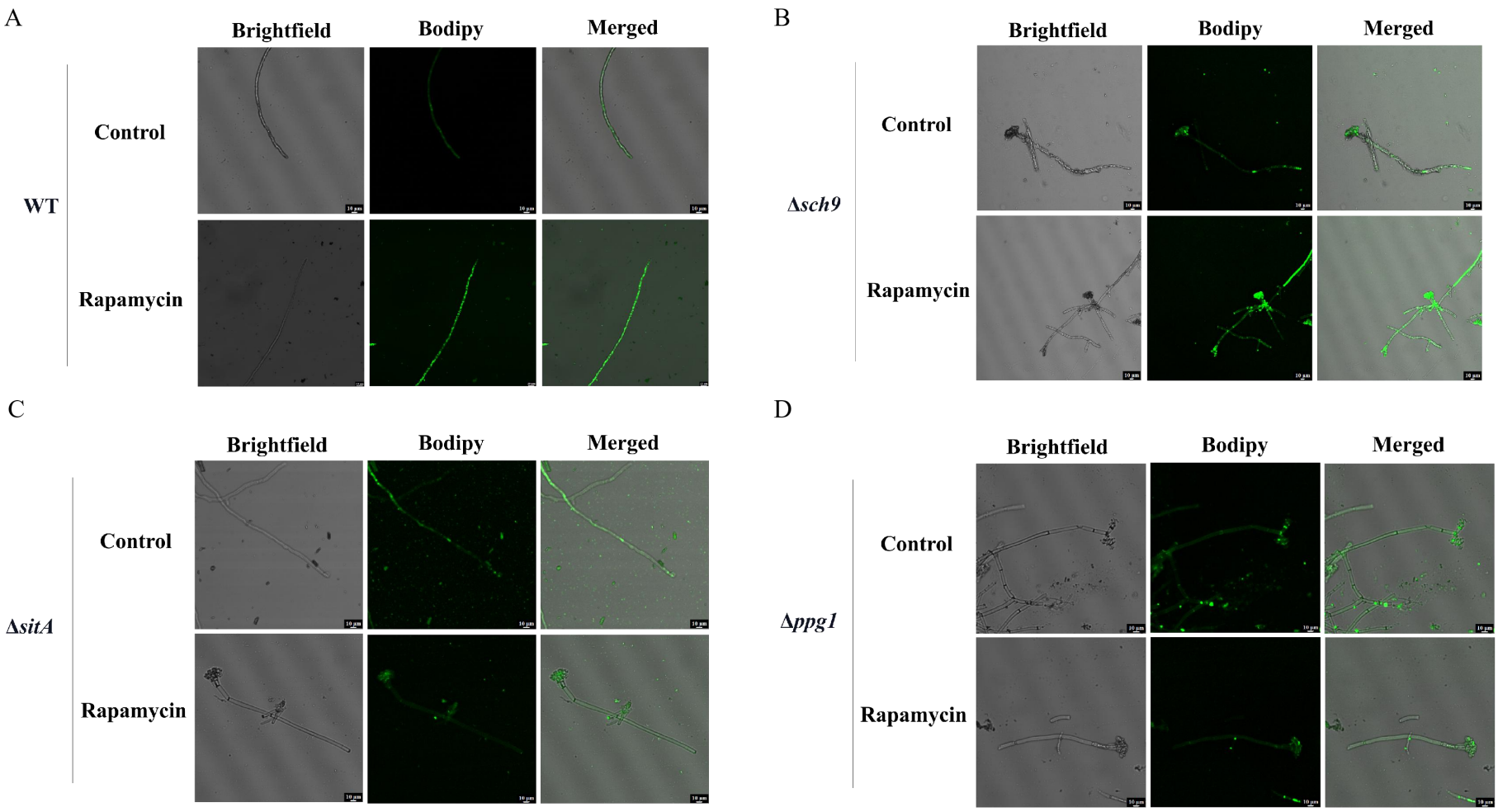
A
Brightfield
Bodipy
Merged
WT
Control
Rapamycin
B
Brightfield
Bodipy
Merged
Δsch9
Control
Rapamycin
C
Brightfield
Bodipy
Merged
ΔsitA
Control
Rapamycin
D
Brightfield
Bodipy
Merged
Δppg1
Control
Rapamycin

Fig. 9 Phosphatase SitA and Ppg1 are involved in regulating lipid droplet biogenesis.

(A) The intracellular lipid droplets were stained by boron dipyrromethene difluoride (BODIPY) in hyphae of the WT strain and observed under fluorescence microscopy. The phenotype of lipid droplets accumulation in the mycelia of the WT strain treated with or without 100 ng/mL rapamycin for 6 h (Bar, 10 μm).

(B) Phenotype of lipid droplets accumulation in the mycelia of the Δ*sch9* strain treated with or without 100 ng/mL rapamycin for 6 h (Bar, 10 μm).

(C) Phenotype of lipid droplets accumulation in the mycelia of the Δ*sitA* strain treated with or without 100 ng/mL rapamycin for 6 h (Bar, 10 μm).

(D) Phenotype of lipid droplets accumulation in the mycelia of the Δ*ppg1* strain treated with or without 100 ng/mL rapamycin for 6 h (Bar, 10 μm).

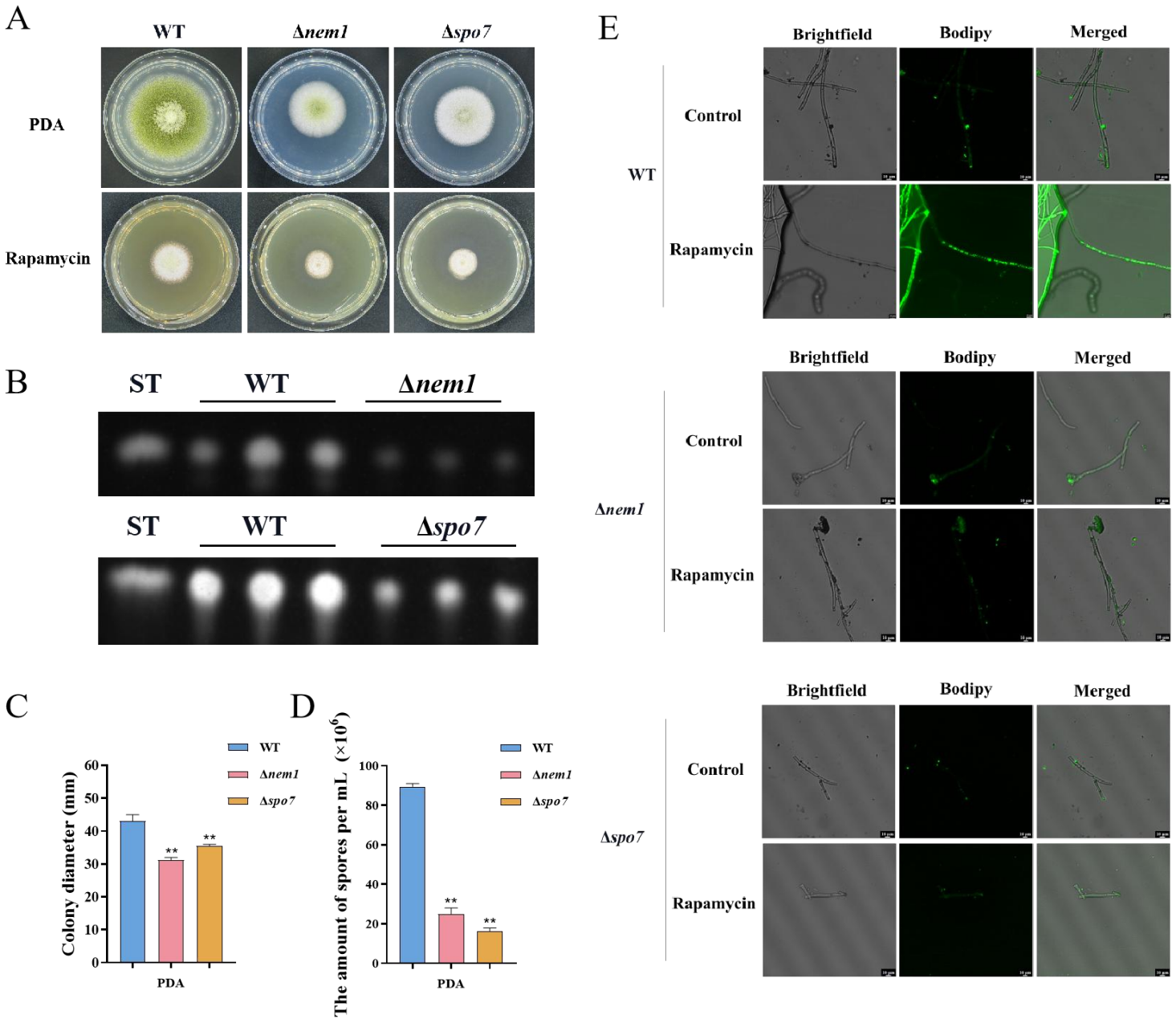
A
WT
Δnem1
Δspo7
PDA
Rapamycin
B
ST
WT
Δnem1
ST
WT
Δspo7
C
Colony diameter (mm)
WT
Δnem1
Δspo7
PDA
D
The amount of spores per mL (×10^6)
WT
Δnem1
Δspo7
PDA
E
Brightfield
Bodipy
Merged
WT
Control
Rapamycin
Δnem1
Control
Rapamycin
Δspo7
Control
Rapamycin

Fig. 10 Phosphatase complex Nem1/Spo7 play significant role in growth, conidiation, aflatoxin, and lipid droplet biogenesis.

(A) Phenotype of the WT, Δ*nem1*, and Δ*spo7* strains grown on PDA amended with 100 ng/mL rapamycin at 37°C for 5 days.

(B) TLC assay of AFB_1 production from the WT, Δ*nem1*, and Δ*spo7* strains cultured in YES liquid medium at 29°C for 6 days.

(C) Growth diameter of the WT, Δ*nem1*, and Δ*spo7* strains on PDA media.

(D) Statistical analysis of the sporulation by the WT, Δ*nem1*, and Δ*spo7* strains.

(E) Phenotype of lipid droplets accumulation in the mycelia of the WT, Δ*nem1*, and Δ*spo7* strains treated with or without 100 ng/mL rapamycin for 6 h (Bar, 10 μm).

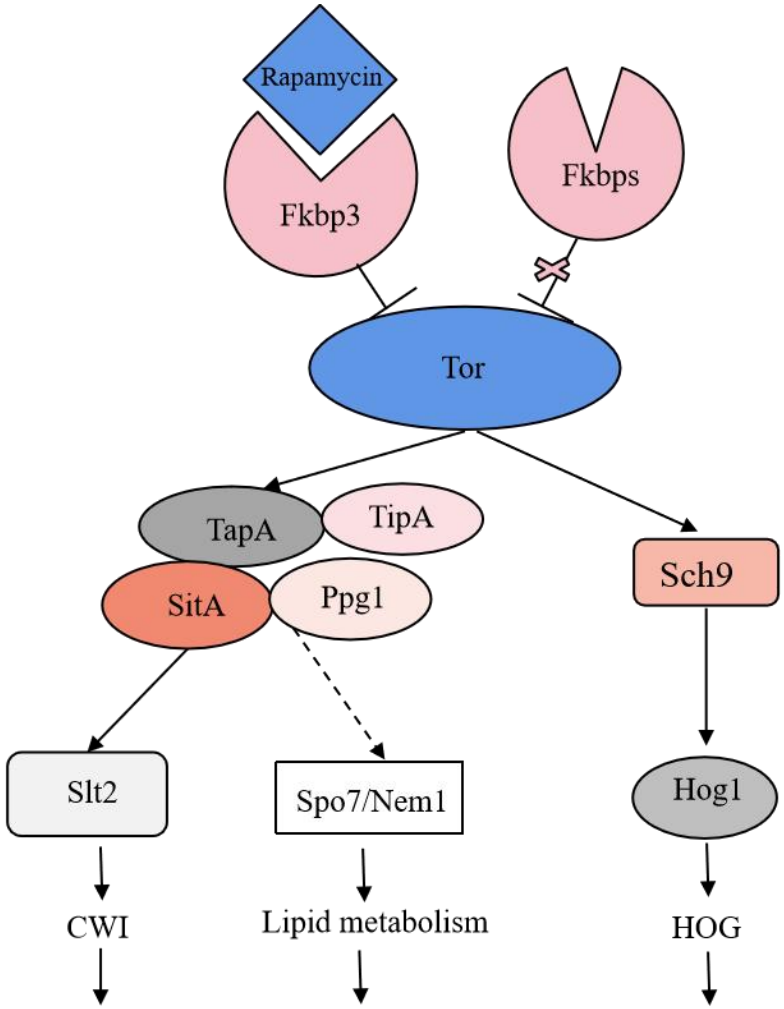

Vegetative development, stress responses, aflatoxin biosynthesis, and pathogenicity.

Fig. 11 The proposed model of the target of rapamycin (TOR) pathway in *A. flavus*.

Based on the above results, we propose a hypothesis regarding the TOR signaling pathway model in *A. flavus.* Rapamycin forms a complex with Fkbp3, and this particular complex can bind to the Tor kinase, thereby impeding its regular functionality. Sch9, functioning as a downstream element of the Tor kinase, regulates aflatoxin biosynthesis and HOG signaling pathway. As another important target of the Tor kinase, TapA-phosphatase complex is involved in the regulation of growth, sporulation, sclerotia, aflatoxin production, CWI signaling pathway, lipid droplet synthesis, and other processes. In conclusion, the TOR signaling pathway plays a crucial role in various aspects of *A. flavus*, including vegetative development, stress response, aflatoxin biosynthesis, and pathogenicity.